NAVAL POSTGRADUATE SCHOOL
Monterey, California

THESIS

ANALYSIS OF JAMMER RESISTANT, SPREAD SPECTRUM, VSAT COMMUNICATION SCHEME FOR MARITIME PLATFORM USING DS-CDMA.

by

Ersin Aras

September 2002

Thesis Advisor:	Tri T. Ha
Second Reader:	Herschel H. Loomis

Approved for public release; distribution is unlimited

THIS PAGE INTENTIONALLY LEFT BLANK

REPORT DOCUMENTATION PAGE			Form Approved OMB No. 0704-0188
Public reporting burden for this collection of information is estimated to average 1 hour per response, including the time for reviewing instruction, searching existing data sources, gathering and maintaining the data needed, and completing and reviewing the collection of information. Send comments regarding this burden estimate or any other aspect of this collection of information, including suggestions for reducing this burden, to Washington headquarters Services, Directorate for Information Operations and Reports, 1215 Jefferson Davis Highway, Suite 1204, Arlington, VA 22202-4302, and to the Office of Management and Budget, Paperwork Reduction Project (0704-0188) Washington DC 20503.			
1. AGENCY USE ONLY *(Leave blank)*	**2. REPORT DATE** September 2002	**3. REPORT TYPE AND DATES COVERED** Master's Thesis	
4. TITLE AND SUBTITLE: Analysis of Jammer Resistant, Spread spectrum, VSAT Communication Scheme for Maritime Platform Using DS-CDMA. (Mix Case Letters)			**5. FUNDING NUMBERS**
6. AUTHOR(S) Ersin Aras			
7. PERFORMING ORGANIZATION NAME(S) AND ADDRESS(ES) Naval Postgraduate School Monterey, CA 93943-5000			**8. PERFORMING ORGANIZATION REPORT NUMBER**
9. SPONSORING /MONITORING AGENCY NAME(S) AND ADDRESS(ES) N/A			**10. SPONSORING/MONITORING AGENCY REPORT NUMBER**
11. SUPPLEMENTARY NOTES The views expressed in this thesis are those of the author and do not reflect the official policy or position of the Department of Defense or the U.S. Government.			
12a. DISTRIBUTION / AVAILABILITY STATEMENT Approved for public release; distribution is unlimited			**12b. DISTRIBUTION CODE**

13. ABSTRACT ***(maximum 200 words)***

In this thesis, a new VSAT (Very Small Aperture Terminal) communication system is developed using Direct Sequence Code Division Multiple Access (DS-CDMA) for multiple maritime mobile users in the footprint of national communication satellites. The Forward Error Correction (FEC) is implemented by applying convolution encoding with soft decision decoding. The worst-case scenario is always considered by placing VSAT system and different types of jammers on the footprint where the minimum signal-to-noise ratio is possible. Using this assumption, the performance of the system is analyzed for different convolution code rates, for a different number of users and for the different jammer powers. The Walsh codes are used to establish an orthogonal cover between CDMA channels in a VSAT. Additionally, spread spectrum is included by PN sequences to ensure as much orthogonal coverage as possible between the VSATs. Also, that spreading is the key to minimizing these hostile jammer effects. After analyzing VSAT system for possible scenario elements, optimum system parameters are introduced for military and civilian applications.

14. SUBJECT TERMS PAGES VSAT, Satellite Communications, CDMA, Spread Spectrum, Performance Analysis, Link Budget, Link Margin, Pulse Jamming, Tone Jamming, Walsh Functions, PN Sequences, Convolutional Codes, Forward Error Correction, Channel Distances, Gaussian Approximation.			**15. NUMBER OF PAGES** 94 **16. PRICE CODE**
17. SECURITY CLASSIFICATION OF REPORT Unclassified	**18. SECURITY CLASSIFICATION OF THIS PAGE** Unclassified	**19. SECURITY CLASSIFICATION OF ABSTRACT** Unclassified	**20. LIMITATION OF ABSTRACT** UL

NSN 7540-01-280-5500 Standard Form 298 (Rev. 2-89)
Prescribed by ANSI Std. 239-18

THIS PAGE INTENTIONALLY LEFT BLANK

Approved for public release; distribution is unlimited

ANALYSIS OF JAMMER RESISTANT, SPREAD SPECTRUM, VSAT COMMUNICATION SCHEME FOR MARITIME PLATFORM USING DS-CDMA.

Ersin Aras
Lieutenant Junior Grade, Turkish Navy
B.S., Turkish Naval Academy, 1996

Submitted in partial fulfillment of the
requirements for the degree of

MASTER OF SCIENCE IN SYSTEMS ENGINEERING

from the

NAVAL POSTGRADUATE SCHOOL
September 2002

Author: Ersin Aras

Approved by: Prof. Tri T. Ha
Thesis Advisor

Prof. Herschel H. Loomis
Second Reader

Dan C. Boger
Chairman, Information Sciences Department

THIS PAGE INTENTIONALLY LEFT BLANK

ABSTRACT

In this thesis, a new VSAT (Very Small Aperture Terminal) communication system is developed using Direct Sequence Code Division Multiple Access (DS-CDMA) for multiple maritime mobile users in the footprint of national communication satellites. The Forward Error Correction (FEC) is implemented by applying convolution encoding with soft decision decoding. The worst-case scenario is always considered by placing VSAT system and different types of jammers on the footprint where the minimum signal-to-noise ratio is possible. Using this assumption, the performance of the system is analyzed for different convolution code rates, for a different number of users and for the different jammer powers. The Walsh codes are used to establish an orthogonal cover between CDMA channels in a VSAT. Additionally, spread spectrum is included by PN sequences to ensure as much orthogonal coverage as possible between the VSATs. Also, that spreading is the key to minimizing these hostile jammer effects. After analyzing VSAT system for possible scenario elements, optimum system parameters are introduced for military and civilian applications.

THIS PAGE INTENTIONALLY LEFT BLANK

TABLE OF CONTENTS

LIST OF FIGURES

LIST OF TABLES

THIS PAGE INTENTIONALLY LEFT BLANK

ACKNOWLEDGMENTS

I want to express my deepest appreciation to my advisor Professor Tri Ha who has been an exemplary teacher, advisor and scholar for the time I have been in Naval Postgraduate School. He has been my teacher, my advisor and a model disciplined academic character for the time I have been at the Naval Postgraduate School.

I must thank my dear wife, Nese, for being so patient over the past four months and for carrying out every responsibility for the care of our beloved newborn son, Burak Selim. My wife's support during my research was priceless because of her unflagging belief that I would succeed in whatever I put my mind to.

In addition, I could not have started or finished this thesis without the support and assistance of my colleague, Ugur Yigit. We were not only a great team but were the best of friends throughout our stay here at the Naval Postgraduate School. We complemented each other, forming a team spirit, which was one of the reasons we were able to finish our thesis work.

I also want to thank Ron Russell for his help in editing my thesis

Finally, I thank Jan Elizabeth Tighe whom I have never met. Yet her dissertation work became a torch, which enlightens my way through my studies that I used whenever I lost my way.

I. INTRODUCTION

A. BACKGROUND

Mankind fought with each other long before recorded history. As the centuries passed, new long-range weapons appeared on battlefields and on seas. Long-range weapons gave opponents ability to hide and to make surprise attacks, but at the same time they created the need to locate the enemy. This need eventually led us to the invention of radar. While World War II was raging in Europe and later in other places as well, the techniques and capabilities of radar usage was upgraded.

The first use of electromagnetic action in history began in World War I and in the Russian-Japanese War, long before the "Electronic Warfare" concept was shaped. On May 31, 1916, Admiral of the British Fleet, Sir Henry Jackson, used coastal radio direction finders to observe movements of the German fleet and, on the basis of this information, positioned the British fleet so that it could oppose the German forces successfully. Earlier use of electromagnetic action is claimed where the Russian torpedo boat *Gromky* and cruiser *Igumrad* jammed Japanese radio communications during the Russian-Japanese War at the Battle of Tsushima in May 1905 [1].

As a principle of radar, the reflected energy that is returned to the radar from a target indicates the presence of a target, but also transmitting such electromagnetic energy reveals presence of a radar to the target. These types of intentional and electromagnetic actions and counter actions occured many times in many campaigns of WWII. Meanwhile, all types of electromagnetic actions began to be called "Electronic Warfare."

The "electronic warfare" concept was shaped during WWII. During the Cold War, the potential effect of Russian EW systems over U.S. weapon systems strengthened the importance of EW. Admiral Thomas H. Moorer, Chairman of the U.S. Joint Chiefs of Staff in 1970-1974, stated, "If there is a WW III, the winner will be the side that can best control and manage the electromagnetic spectrum" [1].

Today we must use the electromagnetic spectrum well and protect our weapon systems from enemy electromagnetic actions to achieve success. A reliable communication is also essential for both sides. Since this communication system uses the electromagnetic spectrum, it will also be targeted by the enemy's electronic warfare capabilities. Until we find another way to communicate other than radio waves, communication signals will intentionally be jammed by the enemy or be interfered unintentionally by friends. At this point, there is an urgent need for a reliable communication system, which can be used in all weather conditions, is endurable against enemy jammer activity, and is difficult for an enemy to intercept.

B. OBJECTIVE

In this thesis, we will design a satellite communication system with a "Very Small Aperture Terminal" (VSAT) that can easily be carried by a naval vessel. This system will serve the naval platforms in the footprint of national communication satellites to carry all of the voice traffic as well as the data. Data traffic will essentially consist of position information of friends and verified enemies, which will be detected by sensors aboard ships or helicopters. Continuous transmission of this valuable information from all platforms in the tactical arena would be important to winning the battle. In some cases, interruption in transmission cannot be tolerated even if Emission Control (EMCON) measures are on progress. Due to the directivity advantage of satellite terminal antennas, a minimum electromagnetic signature would be revealed to the enemy outside of the narrow main beam, so continuous transmission could be established in many cases. To be able to establish a continuous picture of the tactical arena, some technical requirements must be achieved, such as bit rate and bandwidth for desired signal-to-noise plus interference ratio that can be supported by the platform.

This system includes many tools such as Direct-Sequence Code Division Multiplexing Access (DS-CDMA) and convolutional encoding with soft-decision decoding. Different ratio of contributions from spectrum spreading and convolutional encoding for a fixed spreading factor enables us to have a flexible jammer resistant

system against different capabilities of the enemy jammer. Significantly, we will analyze the effect of enemy jammer types on our system and define the capability of this system.

C. RELATED WORK

In this thesis, we mainly studied the performance analysis of spread spectrum satellite communication systems under different jamming conditions. A detailed similar related work was done in [3], studying the *"Modeling and Analyzing of Cellular CDMA Forward Channel."* Also in reference [15], Ugur Yigit has studied the performance analysis of a spread spectrum VSAT system for different coding techniques. Chapter III of this thesis and of reference [15] were written jointly by the author and U. Yigit.

D. THESIS OUTLINE

The main goal in Chapter II is calculating the minimum signal-to-noise ratio that our system can support. Initially, we define the term VSAT and other orbital mechanics parameters. Then we decide on the proposed VSAT system requirements. By using the physical sizes, distances and power limitations, a link budget analysis will be introduced. The worst-case scenario is considered in this analysis assuming a friendly platform at the edge of the satellite footprint and the enemy jammer at the best place to minimize our system's performance. The link budget analysis presents the minimum and maximum signal-to-noise ratios that can be established at the satellite receiver. The difference between the minimum and maximum signal-to-noise ratios will be calculated by the link margin analysis.

In Chapter III, we examine the algebraic properties of the Walsh functions and PN sequences that will help to determine how to minimize jammer effects and friendly interference on our system. We present the extended orthogonality that ensures the orthogonality between every channel in a VSAT and introduce the PN sequences used to spread out our frequency spectrum, reducing the power spectral density and minimizing the jammer effects. Afterwards, we introduce the convolutional forward-error-correction coding, which allows the system perform better with a low signal-to-noise ratio.

The performance analyses will be introduced in Chapter IV. The performance analyses are considered both for tone jammer and pulse jammer. First of all, we develop a signal-to-noise plus interference ratio and the probability of bit error for our DS-CDMA satellite system by using Gaussian approximation. For both jammer cases, co-channel interference, inter-VSAT interference, Additive White Gaussian Noise and Jammer Interference were considered as variances of our random variable Y. In our uplink model, we introduce Forward Error Correction (FEC) in the form of convolutional encoding with soft-decision and develop an upper bound on the probability of bit error [3].

Then, we use a simulation software to analyze the probability of bit error for the minimum signal-to-noise ratio, which will be defined in Chapter II. At the end of Chapter IV, optimal performance parameters will be introduced.

We will summarize the conclusions in Chapter V.

II. VERY SMALL APERTURE TERMINAL

In this chapter, basic satellite communication and VSAT concepts will be introduced. Some necessary parameters in satellite communication and orbital mechanics will be assessed to find the maximum signal-to-noise ratio for the modeled VSAT system. Then rain attenuation will be calculated to decide on the link margin for the minimum uplink signal-to-noise ratio. Minimum and maximum SNR values will be used in Chapter IV to decide on whether reliable communication can be achieved or not. The decision given on reliability was based on the probability of bit error for a given signal-to-noise ratio range. We will accept that the probability of bit error should be below 10^{-6} within minimum and maximum SNR values to establish reliable communication.

A. DEFINITION OF VSAT

Since Marconi made the first radio transmission across the Atlantic in 1901, communication has been one of the fastest developing branches of electrical engineering. If military requirements had not been so vital when radio was invented, we might never have had a chance to use modern communication devices today. Unquestioningly, military needs have led the developments of communication techniques and devices at the times of WWI, WWII, and Cold War.

While communication technology meets the demands of the military and civilian community, each advancement in these technologies encourages the military and civilian sectors to demand even more sophisticated technology. Consequently, new technology continually begets more and more progressive applications. Thus, today, modern military commands, on the field, in the sea, and in the air require that vast packets of data be transferred rapidly (through high bit rates), and further require large bandwidths, mobility, power efficiency, secrecy and durability under friendly or hostile interference.

A dream of communicating with the farthest point on earth or even across the solar system came within reach after the first communication satellite was set in orbit.

VSAT systems are merely a link in this chain. A VSAT system is only an example, which can answer all those requirements listed above.

New developments in military command structure, which now use information and intelligence more than ever before, exchange enormous amounts of data between different commands and units. In peacetime, establishing several communication media that enable such operations is possible. However in a crisis situation, establishing an effective communication system in the field, either in one's own territory or in a foreign country is troublesome to maintain. An affordable solution that can resolve most of these problems is the VSAT.

The term VSAT stands for Very Small Aperture Terminal. VSATs are small ground terminals, which can communicate with a satellite either as a receive-only terminal or a transmit-receive terminal. VSATs provide cost-effective solutions for the growing telecommunication needs throughout the world [10]. Today's satellites are more powerful, enabling the use of smaller and less-expensive antennas on the ground. Also, the developments in silicon technology include most of the necessary VSAT functions, which makes VSATs more effective.

Although there are many definitions for a VSAT, the European Telecommunication Standard Institute has a comprehensive one, which mainly describes a VSAT as part of a satellite transmit-receive system that has an aperture size smaller than $3.8 m^2$ [11].

The main VSAT deployment configurations are the star and mesh configurations. Each system has advantages and disadvantages. For military applications, the mesh structure has more advantages than the star configuration. The central hub in a star configuration would be an important and primary target for an attack, which would cause an overall catastrophe for communication if the central hub were destroyed or were made to malfunction. There is no vital VSAT in the mesh configuration. Therefore, even if the high traffic hubs all malfunctioned, the rest of the system would be able to carry the entire communication load, not through the hubs, but directly from VSAT to VSAT via the communication satellite.

B. LINK GEOMETRY

Today's VSATs are commonly but not necessarily used with geostationary communication satellites. A geostationary satellite always appears to be at the same altitude and azimuth for a particular location on earth. Therefore such a satellite rotates around the earth with a period of one sideral day and with zero inclination with respect to the earth's equator and stays above the same geographical location as the earth rotates at the same velocity as well. The gravitational force upon a body decreases as the distance from the earth increases. The centrifugal force increases upon a body as the velocity of an orbiting body increases. At a certain distance - a point at which the satellite is precisely located - the gravitational pull toward the earth's center and the centrifugal force away from the earth become equal for a circular orbit. This distance is known as geostationary radius, a_{gso}. The geostationary radius is 42,164 km regardless of the size or of the mass of the satellite or orbiting body. The derivation of this distance was given in reference [8]. The geostationary height is found by subtracting the earth's radius from a_{gso}.

$$\begin{aligned} h_{gso} &= a_{gso} - a_e \\ &= 42164 - 6378 \\ &= 35786\,km \end{aligned} \tag{2.1}$$

In the link budget analysis, we will use the slant range from the VSAT to the satellite to calculate the path loss. The geostationary height and the slant range (distance from the satellite to user) are only equal to each other at the sub-satellite point. The sub-satellite point is defined as "the point on earth vertically under the satellite" in reference [8]. The sub-satellite point is the projection point of the satellite on the equator for geostationary satellites. Because of this fact, the geostationary satellite positions are defined as the longitude of the sub-satellite point (f_{SS}).

A worst-case scenario was considered in both the link budget analysis and in the performance analysis. We design the model for the farthest user in the footprint. As shown in the EIRP map (Figure 1), the footprint of Turksat 2-A reaches far beyond the Mediterranean to the Atlantic Ocean. We will set the borders of the coverage area as the 48 dBW transmitter EIRP (where $G/T = 4\,dB/K$ at the receiver) contour for the optimal

usage. We created the optimal contour for the following criteria: the optimum contour must encircle a considerable amount of operational waters for the Turkish Navy with a maximum $(G/T)_{uplink}$ ratio. The 48 dBW contour encircles the Black Sea, the Agean Sea and 90 % of the Mediterranean Sea. In our model the user will be on the 48 dBW contour and be positioned as far west as possible. This position was determined to be $38.00^0\,N - 0^0\,E$ for the position of the earth station ($l_E = 38$ *and* $f_E = 0$).

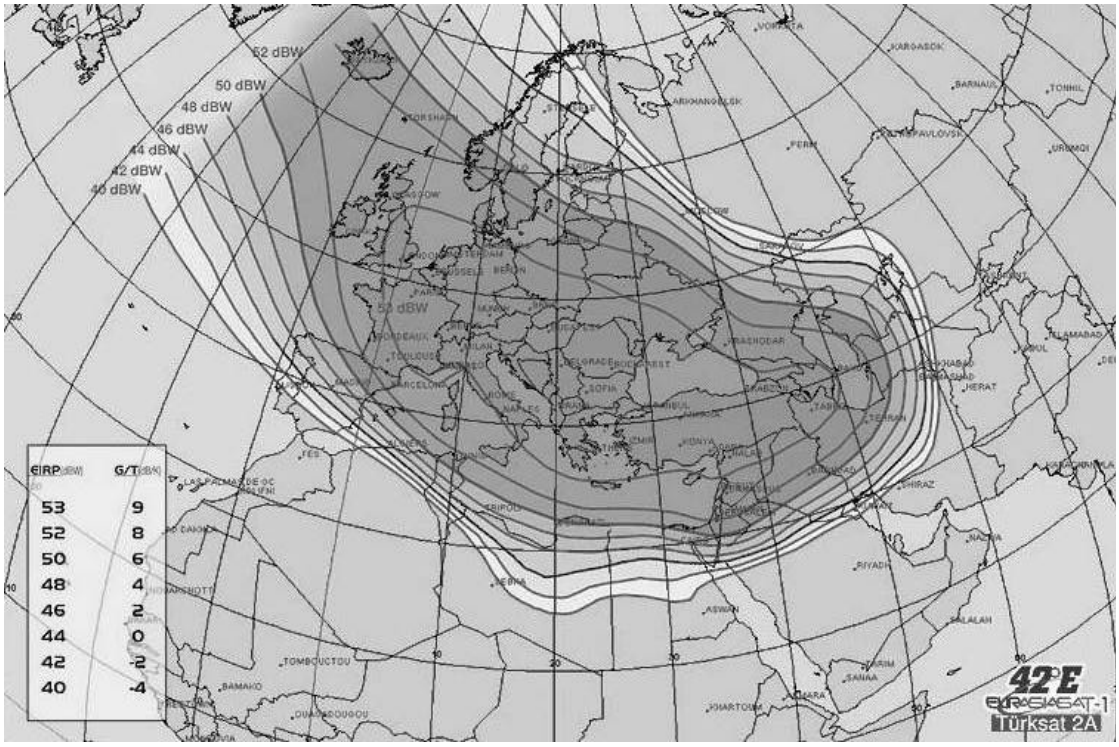

Figure 1. Turksat 2-A West Fixed Beam Footprint and EIRP Map (From [7])

The slant range derivation for $38.00^0\,N - 0^0\,E$ position is introduced as below [8]:

$$d_{sr} = \sqrt{a_E + a_{gso}^2 - 2a_E a_{gso}\cos(b)} \tag{2.2}$$

$$b = \arccos\left(\cos(f_E - f_{SS})\cos(l_E)\right) \tag{2.3}$$

Substituting for b in (2.2),

$$\begin{aligned} d_{sr} &= \sqrt{a_E + a_{gso}^2 - 2a_E a_{gso}\cos(f_E - f_{SS})\cos(l_E)} \\ &= \sqrt{6378 + 42164^2 - 2\times 6378\times 42164\times \cos(0-42)\cos(38)} \\ &= 38247.15\,km. \end{aligned}$$

As seen in the result, the slant range for our particular user is almost 2,500 km longer than the geostationary orbit altitude. This 2,500 km of difference affects the path loss considerably.

C. VSAT SYSTEM REQUIREMENTS

1. Link Budget Analysis

In a possible conflict, such as in the Mediterranean, different types of platforms will be used in the scenario. Each platform will have different communication needs, such as different bandwidths or different bit rates. For instance, a task force would need the sum of all the task group bit-rate requirements in order to relay necessary reports between the task groups and the command base. So this system must be able to serve different platforms, which have different properties.

Older ground terminals used Frequency Modulation (FM) for communication with a satellite. Today, with the advances in digital signal processing, much more effective schemes can be used. These new methods enable increased data rate, increased reliability and efficiency. One particular method is Code Division Multiple Access (CDMA). CDMA allows multiple users to share the same bandwidth and still respond to the varying bandwidth requirements. It also allows integrating the users with small bandwidth requirements into a high data-rate satellite network [12].

Our primary objective is to configure a VSAT (mesh structure) based satellite communication system, which can maintain ship-to-ship, ship-to-shore and shore-to-ship communication via satellite. Because this system is proposed to be on ship, there will be no need to make a power efficient system. But still a tradeoff regarding the power to be used in this system is inevitable. The more power used, the more the bit error rate decreases. On the other hand, the more power used, the more possible interception by an enemy becomes.

Finally, the system should achieve a data rate of at least 6.312 Mbps and must be able to maintain a connection with the satellite under adverse weather conditions and/or jamming. Using spread spectrum techniques enhanced with proper error correction coding algorithms will make our VSAT communication system resistant to friendly interference and hostile jamming. The required signal-to-noise ratio calculation for the uplink without jammer contribution is necessary for the further performance analysis.

A link analysis is given for the uplink according to specifications for Turksat 2-A. We will not need the downlink calculation for the system because the performance analysis will be based on the scenario that the communication satellite is the target to be jammed.

Satellite Name	Turksat 2-A
Origin	Turkey
Mission	Telecommunications
Location	42 E (Geostationary)
EIRP (Fixed West Beam)	53 dBW (Max) 48 dBW (Optimum coverage)
Satellite G/T	9 dB/K (Max) 4 dB/K (Optimum coverage)
Uplink Frequency	17300-18100 MHz
Downlink Frequency	11700-12500 MHz

Table 1. Specifications of Turksat 2-A (From [7])

Proposed VSAT specifications are given in Table 2.

Required Bit Rate	6.312 Mbps (T2)
VSAT Power	150 W
VSAT G/T max	20 dB/K

Table 2. Proposed VSAT Specifications (From [17])

The minimum VSAT Antenna Gain for uplink was found by taking the minimum carrier frequency into account:

$$G_u = \frac{4\pi A_e f^2}{c^2} = \frac{4\pi \times \pi \times 0.8^2 \times 0.55 \times \left(17300 \times 10^6\right)^2}{\left(3 \times 10^8\right)^2} = 46211.71 = 46.64 dB \qquad (2.4)$$

Effective Isotropic Radiated Power:

$$\begin{aligned} EIRP &= P_t G_t \\ &= 150 \times 46211.71 \\ &= 6931757.42 \\ &= 68.41 dB \end{aligned} \tag{2.5}$$

Channel (Path Loss):

$$\begin{aligned} L_c(\text{path loss})_u &= \left(\frac{4p\ fD}{c} \right)^2 \\ &= \left(\frac{4p \times 17300 \times 10^6 \times 38247 \times 10^3}{3 \times 10^8} \right)^2 = 7.68 \times 10^{20} = 208.85 dB \end{aligned} \tag{2.6}$$

The maximum SNR for the uplink at the maximum slant range is;

$$\left. \frac{E_b}{N_o}(dB)_u \right|_{\max} = EIRP(dB) + \frac{G_s}{T_s}(dB) - L_c(dB)_u - L_s(dB) - R_b(dB) + 228.6 \tag{2.7}$$

where L_s : System Losses

System losses include Receiver Feeder Loss (RFL), Antenna Misalignment Loss (AML), Atmospheric Absorption (AA) and Polarization Loss (PL). Assuming the worst scenario, we will accept that $RFL = 2\,dB$, $AML = 1\,dB$, $AA = 2\,dB$ and $PL = 1\,dB$.

Therefore the total system losses will be added to

$$\begin{aligned} L_s &= RFL + AML + AA + PL \\ &= 2 + 1 + 2 + 1 \\ &= 6\,dB \end{aligned} \tag{2.8}$$

The maximum Signal-to-Noise Ratio therefore is

$$\left. \frac{E_b}{N_o}(dB)_u \right|_{\max} = 68.41 + 4 - 208.85 - 6 - 10\log 6.312 \times 10^6 + 228.6 = 18.16\,dB \tag{2.9}$$

2. Rain Loss

The most important reason to look for a suitable rain loss is to ensure that the communication system will be in service without being interrupted due to inevitable events that do not always exist. For example, rain is a factor that must be considered in link margin analysis. The effects of rain are accepted as the major problem in satellite communication at frequencies above 10 GHz [9]. Unlike receiver feeder loss, antenna misalignment loss or polarization loss, rain attenuation is not included in the system losses. All the components in the system's losses can be minimized, even completely eliminated. Conversely rain attenuation is unexpected and inevitable; therefore, it can neither be eliminated nor minimized. Applying a link margin is basically designing the system better than it really needs to be under normal conditions. The designer must be very precise at this stage. Considering uplink, any unnecessary use of sources can cost much and reduce benefits. Considering down link, an unnecessarily established link margin can reduce the satellite's life span and cause the satellite to drop out off service earlier.

Figure 2. Crane Global Model Rain Climate Regions for Europe (From [9])

Figure 2 illustrates the different rain precipitations for different locations in Europe and in the Mediterranean. As we set up our model over maritime conditions, only the Mediterranean and Black Sea will be considered.

Most of the Mediterranean is covered by D_1 region and the Black Sea is covered by F region. Since attenuation is severe in the Mediterranean, D_1 rate distribution values will be used in rain loss analysis.

Rain Rate Exceeded Percent of Year	Point Rain Rate Distribution Values (mm/hr) per Rain Climate Regions			
	D_1	D_2	D_3	F
0.001	90	102	127	66
0.002	72	86	107	51
0.005	50	64	81	34
0.01	37	49	63	23
0.02	27	35	48	14
0.05	16	22	31	8.0
0.1	11	15	22	5.5
0.2	7.5	9.5	14	3.8
0.5	4.0	5.2	7.0	2.4
1.0	2.2	3.0	4.0	1.7
2.0	1.3	1.8	2.5	1.1

Table 3. Point Rain Rate Distributions for the Rain Climate Regions of the Crane Global Model. From ([9])

Rain attenuation is defined in terms of exceeded percentage of the time within a year and the rain rate corresponding to that exceeded period [9]. For instance, rain attenuation is exceeded for 0.1 percent of the time in a year, for a rain rate of 11 mm/hr precipitation. In this case, the rain rate is defined as $R_{0.1}$ where $p = 0.1$.

$$a = a R_p^b \ dB/km \tag{2.10}$$

$$A_p = a R_p^b L_s \ r_p \ dB \tag{2.11}$$

where a and b depend on frequency and polarization. The values of "a" and "b" are published in reference [9]. Considering uplink frequency (17.3 GHz) values of "a" and "b" are $a_h = 0.0367$, $a_v = 0.0335$, $b_h = 1.154$ and $b_v = 1.128$ for 15 GHz. Subscript "h" and "v" are for horizontal and vertical respectively. L_s is the physical distance in the transmission path that radio waves are attenuated. This distance is a function of the antenna look angle and the thickness of the raining layer.

$$L_s = \frac{h_r - h_0}{\sin(El)} \tag{2.12}$$

where

h_r = rainheight

h_0 = VSATheight(sea level)

El = AntennaLookAngleorSatelliteElevation

The rain height can be found in reference [8] as a function of the latitude and the rain rate. In Figure 4.4 of reference [8], the rain height was found 3.5 km for 0.1 % rain rate and latitudes between 30 to 40 degrees.

$$\begin{aligned} El &= \arccos\left(\frac{a_{gso}}{d}\sin\left(\arccos\left(\cos(f_E - f_{SS})\cos(l_E)\right)\right)\right) \\ &= \arccos\left(\frac{42164}{38247}\sin\left(\arccos\left(\cos(-42)\cos 38\right)\right)\right) \\ &= 26.67^o \end{aligned} \tag{2.13}$$

$$\begin{aligned} L_s &= \frac{h_r - h_0}{\sin(El)} \\ &= \frac{3.5}{\sin(26.67)} \\ &= 7.8\,km \end{aligned}$$

Finally, the last term in (2.11) is the reduction factor r_p. The reduction factor is calculated with the equation extracted from reference [9].

$$
\begin{aligned}
r_{0.1} &= \frac{90}{90 + 4L_s \cos(El)} \\
&= \frac{90}{90 + 4 \times 7.8 \cos(26.67)} \\
&= 0.76
\end{aligned}
\tag{2.14}
$$

The common "a" and "b" values can be found as,

$$a_c = \frac{a_h + a_v}{2} = \frac{0.0367 + 0.0335}{2} = 0.0351 \tag{2.15}$$

$$b_c = \frac{a_h b_h + a_v b_v}{2a_c} = \frac{0.0423 + 0.0378}{0.0702} = 1.141 \tag{2.16}$$

Therefore the total rain attenuation is

$$
\begin{aligned}
A_p &= 0.0351 \times 11^{1.141} \times 7.8 \times 0.76\, km \\
&= 3.2\, dB
\end{aligned}
$$

Of course the rain attenuation is not the only factor in the link margin analysis. Water vapor and other gas and particle compounds in the atmosphere effect the link margin. Ippolito has published a detailed study of radiowave propagation in satellite communication in reference [9].

The maximum SNR was introduced in (2.9). The minimum SNR is found by subtracting the rain attenuation from the maximum SNR.

$$
\begin{aligned}
\left.\frac{E_b}{N_o}(dB)_u\right|_{\min} &= EIRP(dB) + \frac{G_s}{T_s}(dB) - L_c(dB)_u - L_s(dB) - R_b(dB) + 228.6 - L_m \\
&= 18.16 - 3.2\, dB \\
&\approx 15\, dB
\end{aligned}
$$

In any unexpected, extraordinary weather conditions, performance becomes worse due to the exceeded link margin tolerances. In such a case, the output power of VSAT can be increased to compensate for the unexpected conditions. For instance, doubling output power increases SNR 3dB. In the presence of a pulse jammer $(E_b / J_0 = 10\,dB)$ for the code rate of $1/4$, a 3dB increase in the SNR would decrease the probability of bit error from 1×10^{-4} to 7×10^{-4}.

D. SUMMARY

In this chapter, we define the term VSAT in antenna size terms. According to the given definition, the satellite communication system must have an antenna smaller than 3.8 m^2 to be called a VSAT. In other words, the antenna diameter should be less than 2.2 m. In the model that we present, the antenna size was 1.6 m in diameter. Naval ships can easily carry and maintain such an antenna.

Additionally we introduced a scenario inside the footprint of the Turksat 2-A communication satellite. A friendly ship was positioned at the edge of the coverage area. Pessimistically, the lowest G/T for the satellite receiver and the farthest slant distance were assumed. System losses were exaggerated and rain attenuation was considered. Thereafter, the signal-to-noise ratio and the rain loss were calculated for given parameters. These calculation results will be used in the performance analysis in Chapter IV. For a reliable voice communication, the probability of bit error of 10^{-3} can be sufficient in civilian use. But in military communication systems, this probability is desired to be lower than 10^{-6}.

In the next chapter the proposed DS-CDMA model will be introduced by comparing the similarities and differences between cellular and satellite communication.

THIS PAGE INTENTIONALLY LEFT BLANK

III. VSAT UPLINK MODEL

In this chapter we will introduce the Walsh functions and PN sequences that will be used in proposed VSAT system together. We will achieve CDMA and rejection of co-channel interference between channels in the same VSAT by using Walsh functions. Likewise, PN sequences will minimize the inter-VSAT interference between the same channel sets that are used in different VSATs. The implementation of this system is presented in Figure 3.

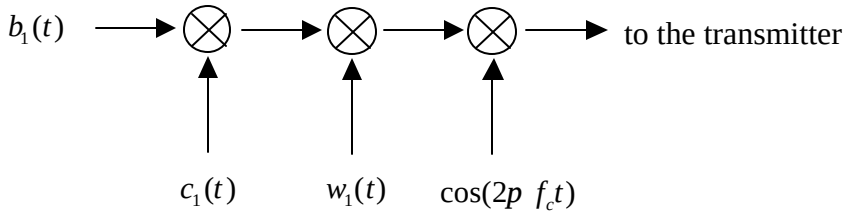

Figure 3. Spreading of Signal with PN Sequences $c(t)$ and Walsh Function $w(t)$

A. WALSH FUNCTIONS COMBINED WITH PN SEQUENCES

Walsh functions mean everything for digital DS-CDMA communication systems, such as satellite or cellular communication. In cellular communication, each unique Walsh code in a Walsh sequence provides orthogonal cover on the forward traffic channel within each cell to eliminate intracell interference. Each mobile user in the cell has a unique Walsh function assigned, which encodes the traffic coming from the base station to the mobile handset. By applying his unique Walsh function to the traffic coming from the base station, the mobile user despreads and, in effect, decodes only the traffic that is intended for a specified user. When his unique code is applied to the remaining intracell traffic in the channel, the orthogonality between user's code and other user codes zeros out their interference. A simplified representation of this process is depicted in Figure 4 [3].

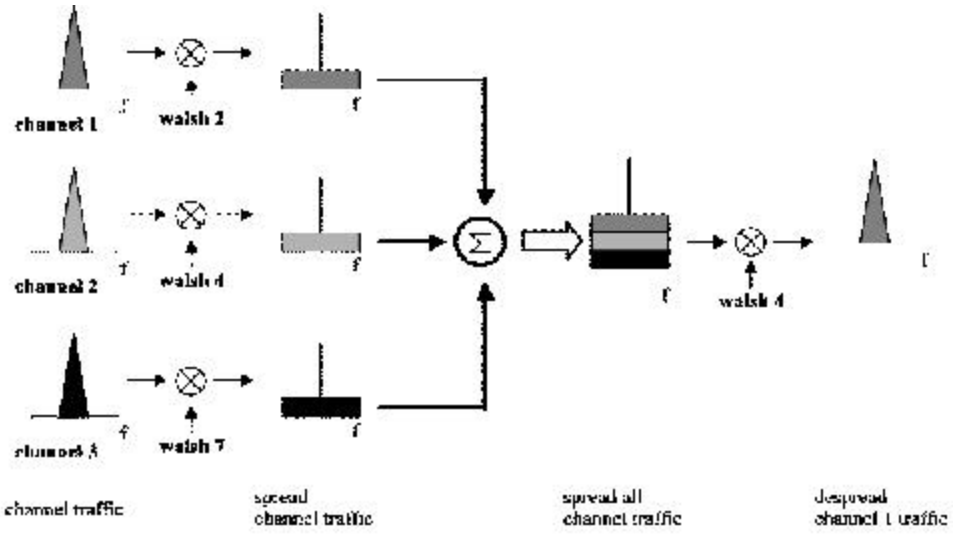

Figure 4. Direct Sequence Spread Spectrum (From [3])

On the other hand, Walsh codes are not the only way to spread the signal. Pseudorandom noise sequences are used to spread the signal as well. Spread Pseudorandom noise is a non-orthogonal function so the coverage supplied by the PN sequence would not be as successful as coverage with a Walsh code. The intracell traffic carrying information for other users would remain spread across the channel's frequency band causing interference for the other users in adjacent cells due to imperfect orthogonality between the cell's PN sequences. How this interference affects the performance of the communication system will be expressed in detail in the next chapter.

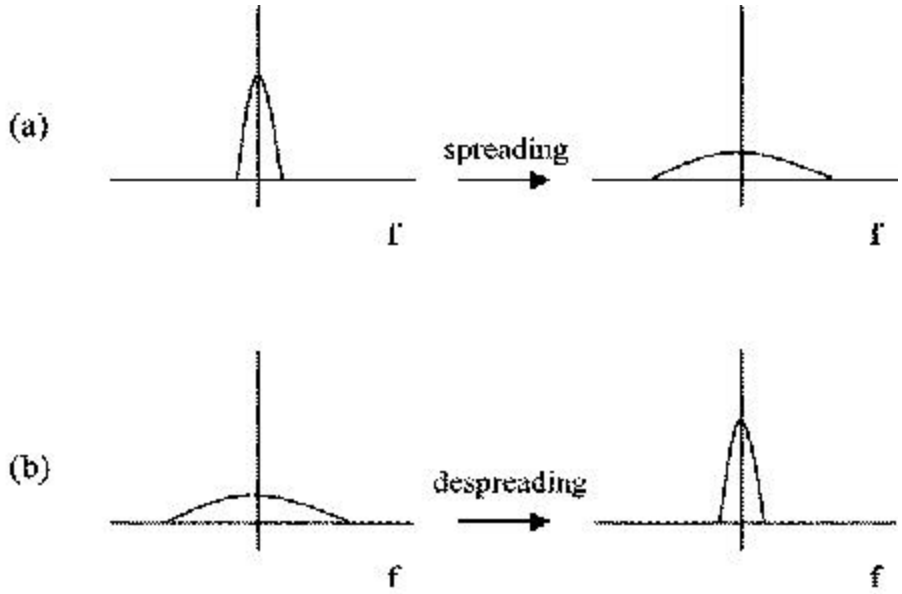

Figure 5. Effect of PN Sequence on Transmit Spectrum

We have introduced an existing example of Walsh codes and PN sequences application, which is cellular communication. Considering the VSAT system, Walsh coding and PN sequences can be applied to satellite communications with some differences in modeling. In cellular communications, every user communicates with his or her own base station in the same cell with different Walsh codes and the same PN sequence. Similarly, in satellite communications, every VSAT communicates with a single communication satellite with one PN sequence but channels separate from each other by Walsh codes. In other words, in a VSAT model every terminal represents cells, which are separated by different PN sequences. Every channel on the single VSAT will be representing users, which are separated by different Walsh Codes.

1. Walsh Codes

Walsh functions have many desirable properties, which we will examine in this section. We will look at their autocorrelation functions, and orthogonality, which are important to the communications engineer.

a. Properties of Walsh Function

Walsh functions are generated from generator matrices, Hadamard matrices, Rademacher functions and Walsh binary index. Orthogonal Walsh functions are

defined in order of N as $W_N = \{ w_j(t); t \in (0,T),\ j = 0,1,..., N-1 \}$, consisting of $N = 2^k$ elements that are functions of time and that have the following properties [13].

- $w_j(t)$ takes on the values $\{+1, -1\}$ except at a finite number of points of discontinuity; where it is defined to be zero.
- $w_j(t) = 1$ for $j = 0$
- $w_j(t)$ has precisely j sign changes in the interval $(0,T)$.
- $$\int_0^T w_j(t)\, w_k(t)\, dt = \begin{cases} 0, & \text{if } j \neq k \\ T, & \text{if } j = k \end{cases} \qquad (3.1)$$

  (Orthogonality Property)

In Figure 6, a set of Walsh functions of order eight has been illustrated for

$$W_8 = \{ w_0(t), w_1(t), w_2(t), w_3(t), w_4(t), w_5(t), w_6(t), w_7(t) \}$$

In this case, the interval $(0,T)$ has been broken into $N = 8$ pieces, each section being $T_c = T / N = T/8$ time units long.

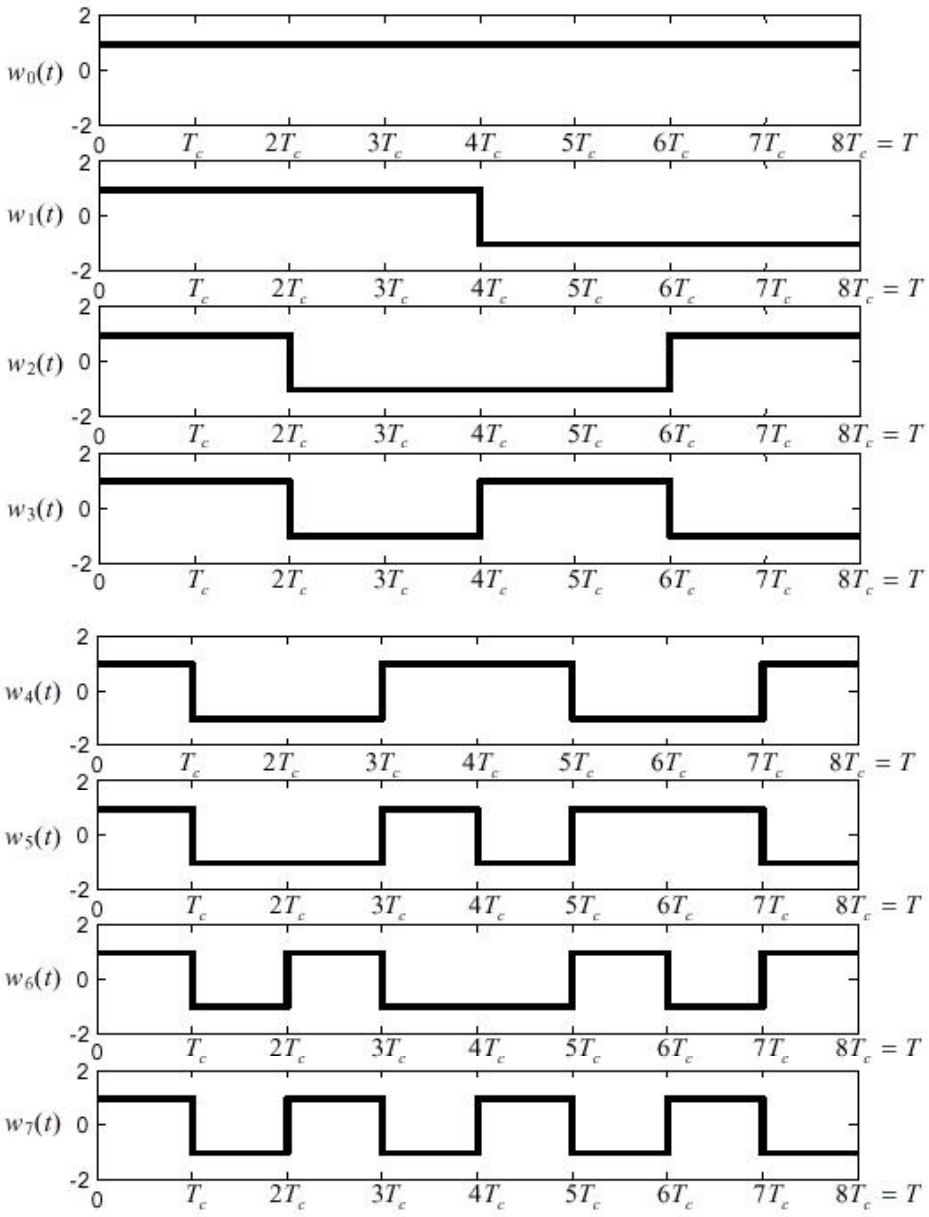

Figure 6. Set of Walsh Function Order Eight (From [3])

The most significant property of the Walsh functions as applied to the DS-CDMA communication systems is that of orthogonality between two different Walsh sequences. We will use this property frequently in our performance analysis. Details about analysis will be introduced in the next section. The orthogonality property implies that the integrating the product of any two different Walsh sequences over a period is always zero. An explanation of the fourth property is depicted below.

$$w_3(t) = [1 \quad 1 \quad 0 \quad 0 \quad 1 \quad 1 \quad 0 \quad 0]$$
$$w_6(t) = [1 \quad 0 \quad 1 \quad 0 \quad 0 \quad 1 \quad 0 \quad 1]$$
$$w_3(t).w_6(t) = [0 \quad 1 \quad 1 \quad 0 \quad 1 \quad 0 \quad 0 \quad 1]$$

Values of "-1" in Figure 6, indicate *logic zero* in this example where *logic one* is indicated with "+1." The product of $w_3(t).w_6(t)$ is calculated by the "*exclusive or*" (XOR) function. The XOR function outputs *logic on*e for the different inputs and *logic zero* for same inputs. Since there are equal numbers of ones and zeros in the product matrix of $w_3(t).w_6(t)$, integration over a period is always zero.

b. Extended Orthogonality

Orthogonality may not always be maintained with three Walsh sequences from a set. The result of the integration of two different Walsh sequences may not be orthogonal to the third Walsh sequence.

$$\int_0^T w_i(t)\, w_j(t)\, w_k(t) = \int_0^T w_k(t) w_k(t) = T \tag{3.2}$$

An example of the situation given in Equation (3.2) is given below for the Walsh function set in Figure 6. Notice that the integration of $w_6(t).w_7(t).w_1(t)$ over a period is "T"

$$w_6(t) = [1 \quad 0 \quad 1 \quad 0 \quad 0 \quad 1 \quad 0 \quad 1]$$
$$w_7(t) = [1 \quad 0 \quad 1 \quad 0 \quad 1 \quad 0 \quad 1 \quad 0]$$
$$w_6(t).w_7(t) = [0 \quad 0 \quad 0 \quad 0 \quad 1 \quad 1 \quad 1 \quad 1]$$
$$w_1(t) = [1 \quad 1 \quad 1 \quad 1 \quad 0 \quad 0 \quad 0 \quad 0]$$
$$w_6(t).w_7(t).w_1(t) = [1 \quad 1 \quad 1 \quad 1 \quad 1 \quad 1 \quad 1 \quad 1]$$

One way around this problem is to diminate some of the Walsh sequences from the complete set of function W_N and force Equation (3.3) to be valid for every Walsh function in the reduced set $\tilde{W}_N$, which we use to define extended orthogonality.

$$\int_0^T w_i(t)\, w_j(t)\, w_k(t) = \int_0^T w_l(t)\, w_k(t) = 0 \tag{3.3}$$

Besides the advantage of establishing orthogonality for every channel on VSAT, reducing the number of Walsh sequences in a set also reduces the number of channels [3]. In extended orthogonality, we will be limiting the number of channels per VSAT. In the real world, some VSAT terminals may require more channels than others do in overall network. In such cases, a greater order of Walsh functions must be used to achieve sufficient number of extended orthogonality Walsh sequences. Then, the system can support a sufficient number of channels. The primary central hubs in the star configuration or the auxiliary hubs definitely need more complex Walsh functions than a remote terminal. Methods for generating a maximum set of extended orthogonality Walsh functions are given in reference [3].

c. Autocorrelation of Walsh Function

In this section, we will examine the autocorrelation functions for the Walsh functions and average autocorrelation for a set of Walsh functions. In order to explore the autocorrelation function of Walsh functions, we will extend our definition and consider each Walsh function to be periodic with a period of T, which is consistent with their use in practice. Each channel on VSAT has a specific Walsh sequence. A satellite onboard processor encodes the data by applying the channel's entire Walsh sequence. The Walsh functions are periodic signals with a period of T. Accordingly, the Walsh function and the corresponding autocorrelation function is also periodic with period T.

We define the normalized autocorrelation function, $a_i(u)$, for any periodic Walsh function $w_i(t) \in W_N$ by

$$a_i(u) = \frac{1}{T}\int_0^T w_i(t)\, w_i(t-u)\, dt. \tag{3.4}$$

Although Equation (3.4) is used for continuous signals, we can consider Walsh sequences as if they were discrete signal. This allows us to generate the autocorrelation of the Walsh functions easily. In spread spectrum systems, the chip duration, T_c, is defined to be the bit duration divided by the number of chips per bit.

$$T_c = \frac{T}{N} \tag{3.5}$$

We will consider T_c as the time increments in discrete Walsh sequences to build the autocorrelation functions. The Walsh function presented in Figure 6 is now presented as the autocorrelation function in Figure 7.

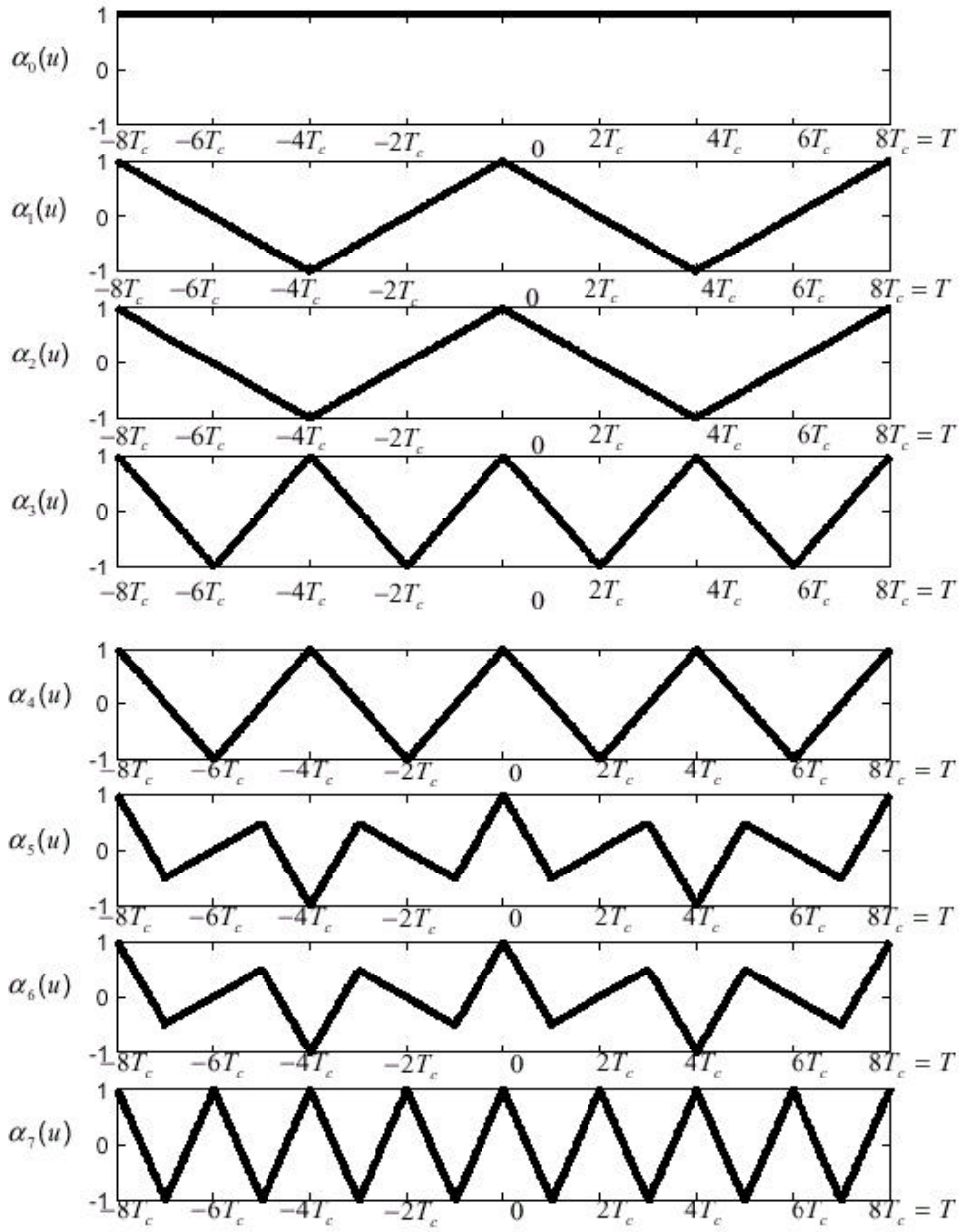

Figure 7. Set of Autocorrelation Function for W_8 (From [3])

The superposition of all the autocorrelation sequences in Figure 7 divided by N gives the "Average Autocorrelation Function" as:

$$A_N(u) = \frac{1}{N}\sum_{i=0}^{N-1} a_i(u) \tag{3.6}$$

where $a_i(u)$ was defined in (3.4). The average autocorrelation function of W_8 is generated from (3.6).

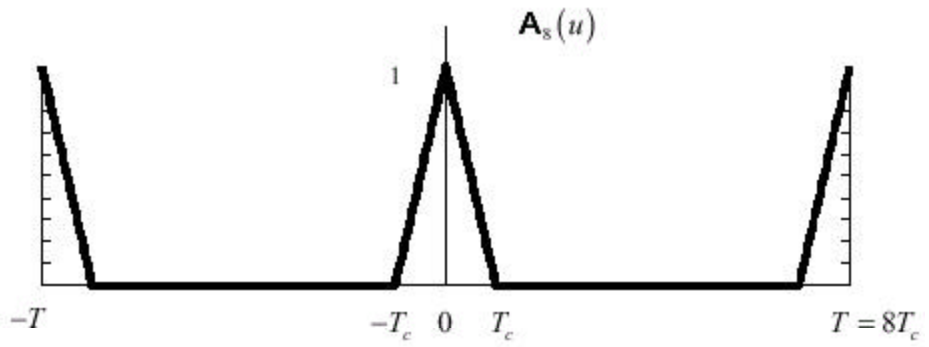

Figure 8. Average Autocorrelation Function, $A_8(u)$ for the set W_N (From [3])

We find that the form of $A_8(u)$ is similar to the form of the autocorrelation function for a random binary signal. A random binary signal is generated from an infinitely long binary random sequence in which the bits are independent and identically distributed random variables. The resulting normalized autocorrelation function for the random binary signal is defined after [13] by

$$b(u) = \begin{cases} 1 - \dfrac{|u|}{T_c}, & |u| \le T \\ 0 & otherwise \end{cases} \tag{3.7}$$

.

2. PN Sequences

A pseudorandom noise (PN) sequence is a sequence of binary numbers, which appears to be random, but in fact is perfectly deterministic. The PN spreading on the uplink provides near-orthogonality and, hence, minimal interference between signals

from each channels sets from different VSATs. This allows reuse of the band of frequencies available, a major advantage of the CDMA. The Direct Sequence Spread Spectrum (DSSS) uses a secondary modulation, faster than the information bit rate, to spread the frequency domain content over a larger band. The spreading process not only assures the system to be more jammer resistant, but also ensures it not to be detected by enemy interceptors. The Low Probability Intercept (LPI) systems use spread spectrum as well. In DSSS, each data bit is modulated by a Pseudonoise (PN) sequence that accomplishes the spectral spreading. The PN sequence consists of random-like plus and minus ones, which are called "chips." Each data bit is modulated with at least 11 to 16 chips. Therefore modulated data bits seem like PN sequences in time domain after being modulated.

a. Properties of PN Sequences

The ratio of data bit intervals to the chip durations are known as processing gain. The higher the processing gain, the better the autocorrelation properties, and hence, the better the ability to reject narrowband interference. In Figure 9-a PN sequence modulates the data bits, 1 0 1 0, (Figure 9-b), resulting in the modulated data bits in Figure 9-c.

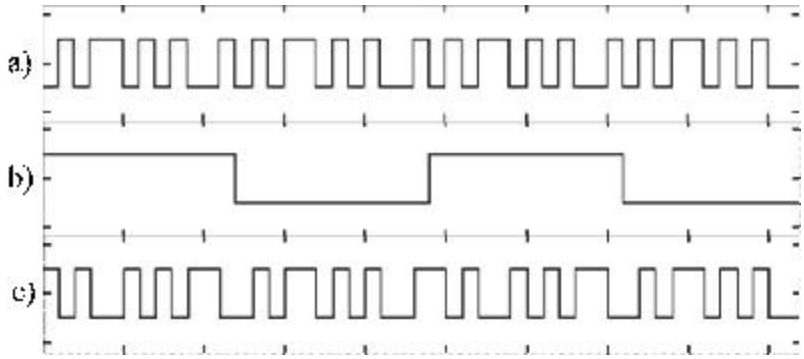

Figure 9. Modulation with PN Sequence

In this example, the processing gain is calculated as 13 because there are thirteen chips per bit. The demodulation process is established in the satellite receiver by applying the exact PN sequence at the correct time (Figure 10). The timing process will be introduced in the following section.

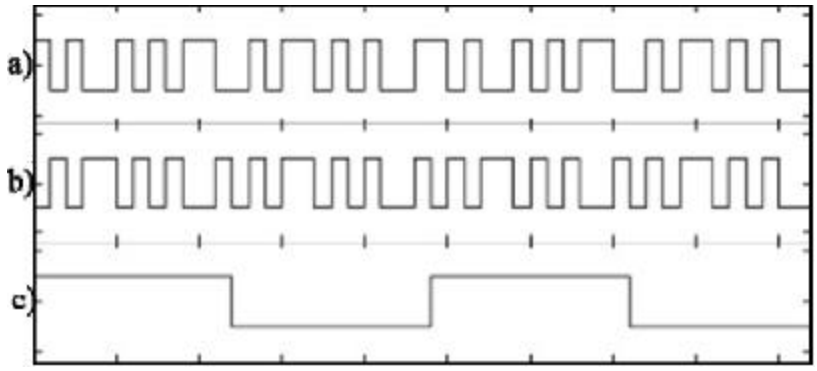

Figure 10. Correct Demodulation with PN sequence

Data bits (1 0 1 0) were recovered after the applying the PN sequence to the modulated data bits. Figure 9 has illustrated the time domain characteristics of a DS Spread Spectrum signal. The frequency domain representation is given Figure 11. The over modulation of the data signal leads to a lower power spectral density covering a larger frequency band. Suppose the spread signal is transmitted in the presence of a narrowband jammer, the despreading operation at the receiver will take the wide band spread spectrum signal and collapse it back to the original data bandwidth. The receiver will also act on the narrowband jammer so that its spectrum is spread and causes much lower interference to the despread signal. This is known as jamming resistance or the natural interference immunity of spread spectrum signals.

We can see that DS Spread Spectrum is bandwidth inefficient in that it uses N chips to transmit a single bit of information. Without spreading the spectrum, we could have transmitted N bits in the same bandwidth. This inefficiency is the tradeoff to achieve interference rejection, or the ability to have reliable communications even in the presence of an interfering signal, such as a jammer. It also reduces the power spectral density of the transmitted signal so that its transmission causes less interference in other systems operating at the same time on the same frequency band.

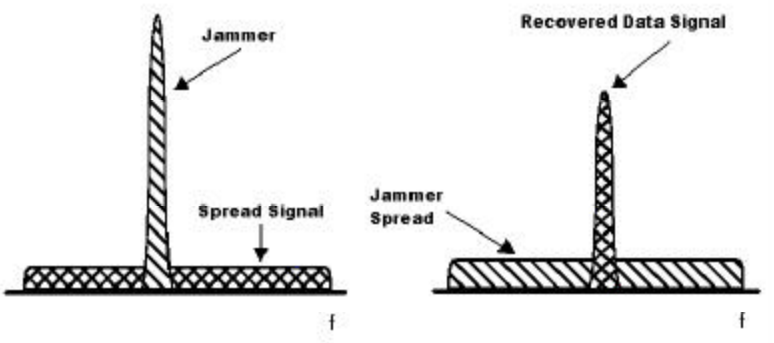

Figure 11. Direct Sequence Spread Spectrum

b. Autocorrelation of PN Sequence

PN sequences have good autocorrelation properties to allow the receiver to recover bit timing and to synchronize the receiver with the uplink. In satellite communication, we expect the users transmit spontaneously without any synchronization between platforms. In such a case, a satellite receiver must apply the Walsh Sequence and PN sequence in the exact time not to allow phase difference between the incoming signal and the demodulation signals. The satellite receiver decides the perfect timing by using the autocorrelation of the incoming signal. The autocorrelation function outputs the peak value at the moment of the correct timing. Figure 9 has illustrated the recovering data signal by applying the correct PN sequence without any phase difference. If the receiver did not apply the correct timing to demodulate the incoming signal, the data would not be recovered.

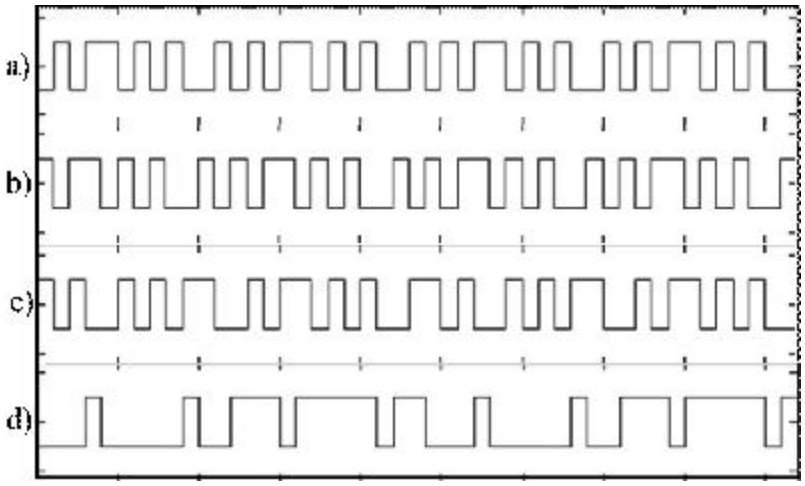

Figure 12. Incorrect Demodulation of Data Signal

An illustration of such a case is given in Figure 12. In part a) is the PN sequence that is used in Figure 9. Instead of multiplying the PN sequence (Figure 12-a) and modulated data bits (Figure 12-c), we multiply the shifted version of the PN sequence (Figure 12-b). The shifted version of the PN sequence was derived by shifting the PN sequence one chip left (early). The result was plotted in Figure 12-d. The decision mechanism after the PN demodulation is different from the demodulation with the Walsh functions. Due to perfect orthogonality, the integration of the demodulated signal over a period has given either zero or one as the decision statistic. However, the PN sequences do not support full orthogonal coverage. Therefore, we must use a decision mechanism other than the one in the Walsh function. We check the after demodulation-integration results with a predefined threshold, which is zero, to decide on the data bit. Although the transmitted and modulated data sequence was (1 0 1 0), the decision is made as (0 1 0 1) after the integration in the example given in Figure 9.

B. CONVOLUTIONAL CODING AND ENCODING [15]

The digital communications itself is prone to errors. The information transferred between the satellite and earth stations is affected by external factors and depending on the signal strength, errors are introduced. The amount of error that can be tolerated depends on the application. For voice communications, bit error rates (BER) up to 10^{-3} can be acceptable, but data communications require BER of at least 10^{-6}. Using higher signal power can increase the performance, but this itself alone is not enough to correct all the errors. Also, the high power may not be available everywhere and the non-linearities in amplifiers limit the output power. Because of these reasons, error correction mechanisms are used.

The principle of error correction coding is adding redundant bits to the information bits and using these redundant bits to detect and correct the errors at the receiver.

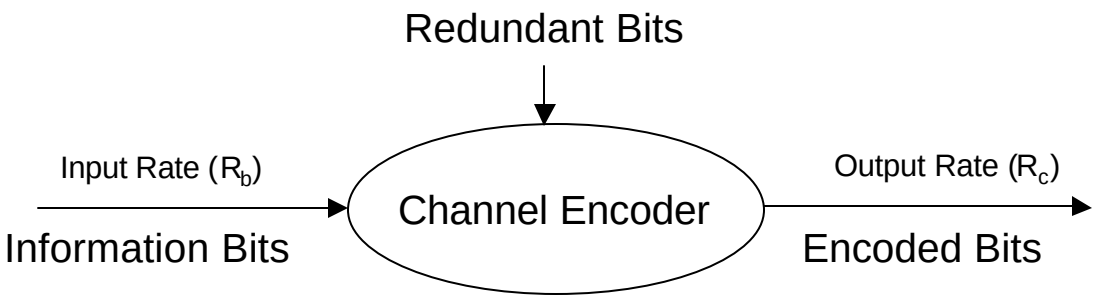

Figure 13. Convolutional Encoding

The code rate is defined as:

$$r = \frac{k}{n} \tag{3.8}$$

n : Number of encoded bits

k : Information Bits

Therefore, in a coded system, there are $(n-k)$ redundant bits. The coding is usually introduced before the modulation in the transmitter, and decoding is done after the demodulator at the receiver. In 1948, Shannon demonstrated that by proper encoding, errors in the received sequence could be reduced to a desired level without sacrificing the rate of information transfer. Provided that for an AWGN channel, Shannon's capacity formula is

$$C = B \cdot \log_2\left(1 + \frac{P}{N_0 B}\right) = B \cdot \log_2\left(1 + \frac{S}{N}\right)$$

C : Channel Capacity (bits per second)

B : Transmission Bandwidth (Hz)

P : Received Signal Power (W)

N_0 : Single-Sided Noise Power Density (W/Hz)

$$\frac{C}{B} = \log_2\left(1 + \frac{R_b E_b}{B N_0}\right) \tag{3.9}$$

where $P = E_b R_b$ and C/B is the bandwidth efficiency.

There are two methods for coding: Convolutional Coding and Block Coding. The block codes are linear and calculate the output frame by depending on the current input frame only, so each block is coded independently of the others and it has no memory. The convolutional codes store the memory of previous input frames and use this to encode the current input frame. Convolutional codes have finite memory and they are linear also.

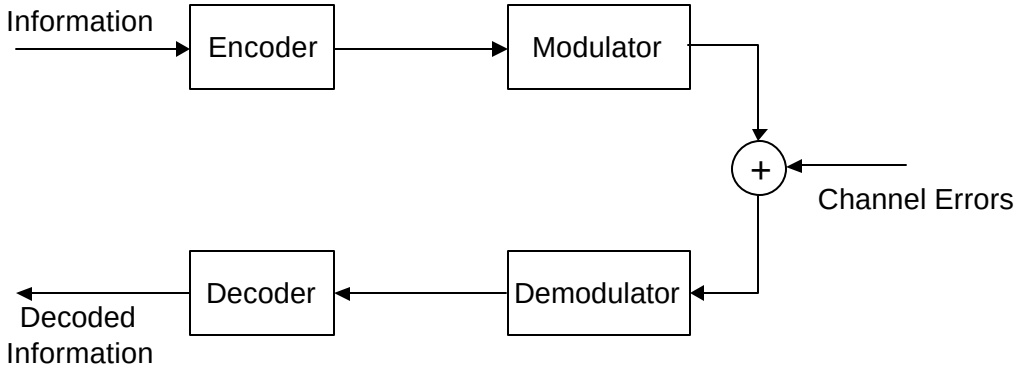

Figure 14. Encoding and Decoding Process

The errors can be corrected once they are detected. The detection of errors is achieved by the redundant bits. Once the error is detected, it can be corrected in several ways. The most common methods are "Error Concealment," "Automatic Repeat Request" (ARQ) and "Forward Error Correction" (FEC).

FEC tries to recover the original information from the received data. A simple example of a (5, 2) block code can be used to demonstrate the FEC:

Information	**Code**
00	00000
01	01011
10	10101
11	11110

Table 4. Encoding

A look-up table or a logic construction can be used to implement the values. In the Table 4, at least three bits would have to change in any code sequence to produce another code sequence. Therefore, this code has a minimum distance of three.

When a code sequence is received, it is verified for its correctness. If there are errors in this received sequence, the code compares it with other sequences and tries to correct it. It is clear that the code can easily correct 1-bit errors. For example, if the transmitted sequence was 01011 and it is received as 01001, the received sequence will have a difference of one bit from 01011, two bits from 00000, and three bits from 10101 and 11110. Thus, it can be corrected as 01011. On the other hand, 2 bits of error will be closer to another sequence, and it will be miscorrected by the decoder. In some cases, the detector can recognize that more than one error has occurred and declare that there are uncorrectable errors. The FEC can be used with other correction mechanisms in conjunction, resulting in even lower error rates.

The cost of error correction coding is the decrease in the information bandwidth. If we represent the uncoded bit rate as R_b and the coded bit rate as R_{coded}, the code rate is:

$$\frac{R_b}{R_{coded}} = r_c$$

r_c is always less than 1. For constant carrier power, the bit energy is inversely proportional to bit rate. Therefore,

$$\frac{E_b}{E_{coded}} = r_c$$

for BPSK modulation, the BER is

$$P_{e,uncoded} = Q\left(\sqrt{\frac{2E_b}{N_0}}\right)$$

For a coded bit stream

$$P_{e,coded} = Q\left(\sqrt{\frac{2r_cE_b}{N_0}}\right)$$

This shows that P_{ecoded} is larger than the $P_{euncoded}$, i.e. the probability of bit error with coding is worse than without coding. However, this is the error rate at the input of the decoder. When the demodulated bit streams are fed into a decoder, some of these errors will be corrected and there will be a coding gain.

A convolutional code is generated by passing the information bits through a finite state shift register. The shift register consists of N (k-bit) stages and n linear algebraic function generators, as shown in Figure 15. The input data is shifted into and along the register, k bits at a time. The number of output bits for each k bit input data sequence is n bits. The number N, called the "constraint length," indicates the number of input data bits the current output is dependent upon. The constraint length determines the complexity and the power of the code. Convolutional codes can be described by their generator matrices, tree diagrams, trellis diagrams or state diagrams.

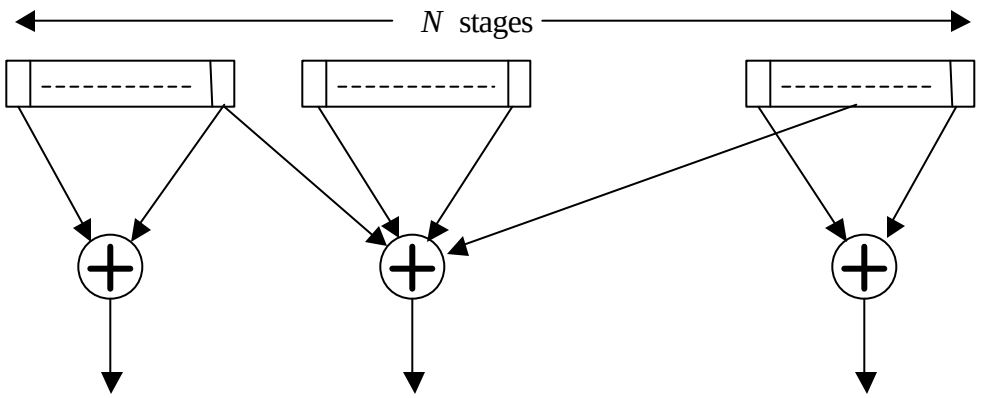

Figure 15. Encoded Sequence (N Bits)

Decoding of convolutional codes is a more difficult problem than encoding. The function of a convolutional decoder is estimating the encoded input information using a method that results in the minimum possible number of errors. Unlike a block code, a convolutional code is a finite state machine. Therefore, the output decoder is a "maximum likelihood estimator" and optimum decoding is done by searching through the

trellis for the most probable sequence. Depending on whether hard decision or soft decision decoding used, either Hamming or Euclidian metric is used, respectively.

Rappaport has given the following definition in [16] for the Viterbi algorithm, which is valid for both hard and soft decision decoding:

> Let the trellis node corresponding to state S_j at time *i* be denoted $S_{j,i}$. Each node in the trellis is to be assigned a value $V(S_{j,i})$ based on a metric. The node values are computed in the following manner:
>
> 1. Set $V(S_{0,0}) = 0$ and $i = 1$
>
> 2. At time *i*, compute the partial path metrics for all paths entering each node.
>
> 3. Set $V(S_{j,i})$ equal to the smallest partial path metric entering the node corresponding to state S_j at time *i*. Ties can be broken by previous node choosing a path randomly. The non-surviving branches are deleted from the trellis. In this manner, a group of minimum paths is created from $S_{0,0}$.
>
> 4. If $i < L + m$, where *L* is the number of input code segments (*k* bits for each segment) and *m* is the length of the longest shift register in the encoder, let $i = i + 1$ and go back to step 2.
>
> Once all the node values have been computed, start at state S_0, time $i = L + m$, and follow the surviving branches backward through the trellis.
>
> The resultant path is the decoded output for the input stream.

C. SUMMARY

In this chapter, we introduced three types of coverage over our satellite uplink transmission. The Walsh functions supply full orthogonal coverage, which is capable of eliminating all inter-VSAT interference in the uplink. The only problem with the Walsh coverage is the possibility of having a non-zero result for the more than two sequence's product integration. The extended orthogonality method compensates for this weak side in the Walsh coverage with an expense of a less number of usable Walsh sequences.

Modulating the uplink signal with a PN sequence makes our system spread in spectrum and ensures the system can resist interference. As an effect of spectral spreading, low power spectral density prevents the VSAT system from being intercepted by enemy ESM capabilities. Even though the PN sequence does not support full

orthogonal coverage, it prevents the interference between different VSATs, which are using the same set of Walsh functions. However, completely eliminating interference between the channels using the same Walsh sequence in different VSATs is not possible.

The coverage with the PN sequences also establishes a processing gain, also called the PN sequence spreading factor. Multiplying the PN sequence spreading factor with the processing gain from the convolutional coding results in the overall spreading factor of our proposed system. We have previously stated that the overall spreading factor of the uplink was 256.

Digital communication systems are subject to noise due to natural reasons. Error correction mechanisms can reduce the required signal-to-noise ratio for a desired BER. There has always been a tradeoff between the coding gain and the bit-rate. System designers must chose the most appropriate code rate and bit-rate pair according to their requirements. We introduce a variable code rate, which can be compensated with processing gain from PN spreading.

We present the connections between Spread Spectrum Systems, Walsh Sequences and Orthogonality, PN sequences and Error Correction Coding in this chapter. When all of them are combined, a robust and high performance system can be designed. The next chapter analyses a system that uses all these components.

THIS PAGE INTENTIONALLY LEFT BLANK

IV. PERFORMANCE ANALYSIS OF DS-CDMA SATELLITE UPLINK

This chapter examines two types of jammer effects over a VSAT system. These are pulse jammer and tone jammer. We will introduce the probability of bit error solution for a spread spectrum VSAT system using convolutional coding. According to these solutions, performances of a VSAT system against different jammer types will be compared.

A. PERFORMANCE ANALYSIS WITH TONE JAMMER

A tone jammer transmits an unmodulated carrier with power J somewhere in the spread spectrum signal bandwidth. The one-sided power spectral density of tone jammer is shown in Figure 16. The single-tone jammer is important because the jamming signal is easy to generate and rather effective against direct sequence spread spectrum systems. Analyzing this jammer with coherent SS systems shows that the jammer tone should be placed at the center of the SS signal bandwidth to achieve maximum effectiveness [2].

As we indicate the similarities and differences of cellular and satellite communication, the total number of M VSATs carrying K channels are placed in footprint of a communication satellite (Figure 17). The number of channels per VSAT is not a fixed number for each VSAT system. Some of the terminals can have less or more channels than the majority according to tactical needs. Besides the VSATs in the footprint, a hostile jammer will be in the middle of the footprint to achieve a maximum effect on our communication system. In this worst-case scenario, we will assume that our friendly VSATs are placed at the edge of the footprint where the sensitivity of the receiver is least.

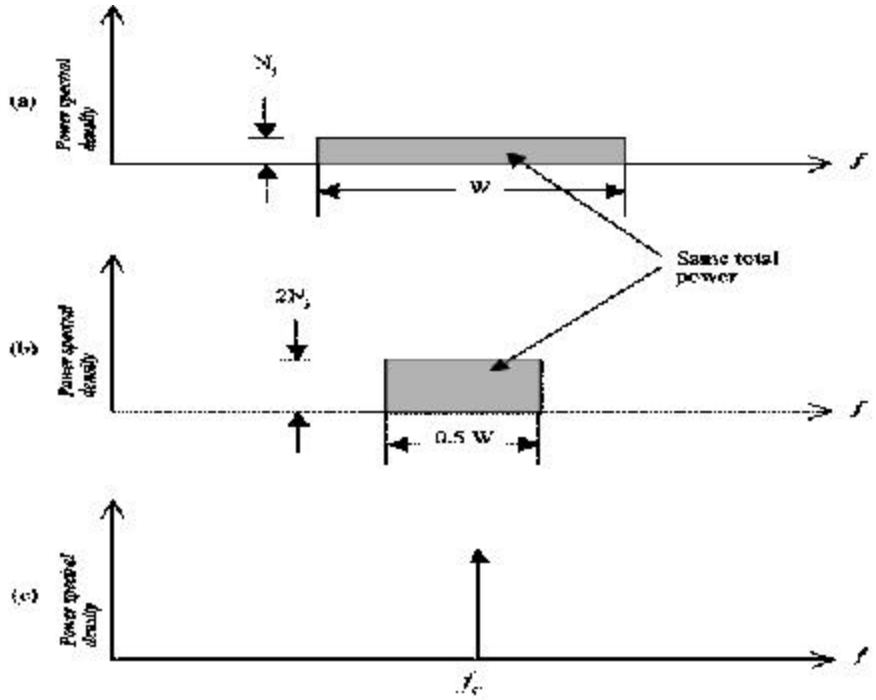

Figure 16. Typical Jammer One-sided Power Spectral Densities (From [2])

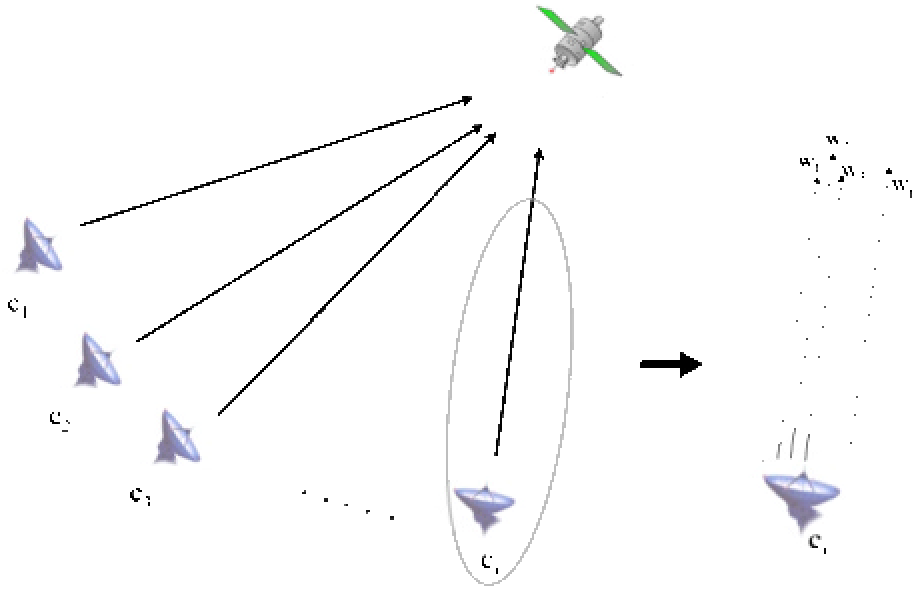

Figure 17. Multi-channel Allocation

We will attempt to recover the information bits $b_1(t)$ from a specified channel ($k=1$) on a VSAT ($i=1$). The received signal from all channels and VSATs will be despread, demodulated and finally integrated over the bit to form a decision statistic, Y. A single tone at the carrier frequency is used for coherent detection and for extracting the demodulated signal, $y_2(t)$ [3].

$$r(t) = S_0(t) + n(t) + V(t) + J(t) \tag{4.1}$$

where,

$S_0(t)$: Information + Co-channel Interference,

$$S_0 = I_0 + g_0 \tag{4.2}$$

$n(t)$: Additive White Gauissian Noise

$V(t)$: Inter-VSAT Interference

$J(t)$: Jammer Interference

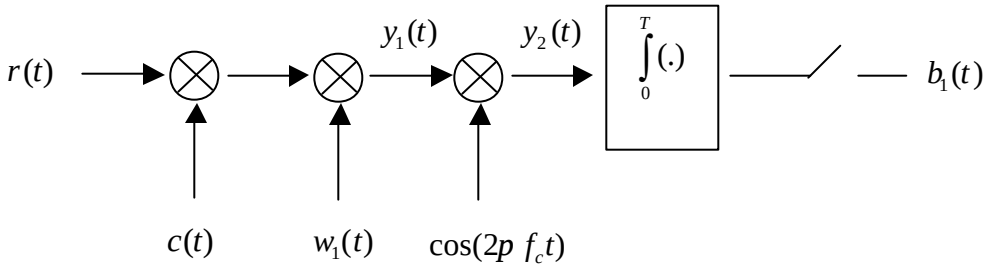

Figure 18. Despreading and Coherent Detection of Incoming Signal from VSATs

1. The Despread Signal, $y_1(t)$

The despread signal is obtained by applying the appropriate PN sequence, which is synchronized with the transmitting VSAT. Synchronization is made by using the autocorrelation function of the PN function, as described in Chapter III. The next step in the despreading is applying the Walsh sequence in order to remove the orthogonal cover as well as to remove spreading.

$$y_1(t) = r(t)\,c(t)\,w_1(t)$$

$$y_1(t) = S_0(t)\,c(t)\,w_1(t) + n(t)\,c(t)\,w_1(t) + V(t)\,c(t)\,w_1(t) + J(t)\,c(t)\,w_1(t) \tag{4.3}$$

The equation above can be simplified as follows: The subscript "1" indicates the despreading.

$$y_1(t) = I_1(t) + g_1(t) + n_1(t) + V_1(t) + J_1(t)$$

$$I_1(t) + g_1(t) = \sum_{k=0}^{K-1} \left(2P_k b_k(t) w_k(t) \cos(2\pi f_c t)\right) c(t)\,w_1(t) \tag{4.4}$$

where

P_k : Received power from k^{th} channel

$b_k(t)$: Information bits for k^{th} channel

$w_k(t)$: Walsh Code for k^{th} channel

In (4.4), $k = 1$ defines the despread information bits that are meant to be recovered from channel. All the other possibilities ($k \neq 1$) will be considered as despread co-channel interference.

$$\begin{aligned} I_1(t) &= \sqrt{2P_1}\, b_1(t) w_1(t) c(t) \cos(2\pi f_c t)\, c(t)\, w_1(t) \\ &= \sqrt{2P_1}\, b_1(t) \cos(2\pi f_c t) \end{aligned} \tag{4.5}$$

$$\begin{aligned} g_1(t) &= \left(\sum_{\substack{k=0 \\ k\neq 1}}^{K-1} \sqrt{2P_k}\, b_k(t) w_k(t) c(t) \cos(2\pi f_c t) \right) c(t)\, w_1(t) \\ &= \sum_{\substack{k=0 \\ k\neq 1}}^{K-1} \sqrt{2P_k}\, b_k(t) w_k(t)\, w_1(t) \cos(2\pi f_c t) \end{aligned} \tag{4.6}$$

Despread Additive White Gaussian Noise,

$$n_1(t) = n(t)\,c(t)\,w_1(t) \tag{4.7}$$

Even though each VSAT has been separated by different PN sequences, the interference between VSATs is unavoidable due to imperfect orthogonality of PN functions. Interference increases as the number of active VSATs (denoted as M) is increased. Interfering channels from different terminals will possibly contain different phase information (θ_i) from the channel, which is intended to be recovered in our analysis.

$$\begin{aligned} V_1(t) &= \left(\sum_{i=1}^{M} \sum_{k=0}^{K_i-1} \sqrt{2P_{ik}}\, b_{ik}(t+\tau_i)\, w_{ik}(t+\tau_i)\, c_i(t+\tau_i) \cos(2\pi f_c t + \theta_i) \right) c(t)\, w_1(t) \\ &= \sum_{i=1}^{M} \sum_{k=0}^{K_i-1} \sqrt{2P_{ik}}\, b_{ik}(t+\tau_i)\, w_{ik}(t+\tau_i) w_1(t)\, c_i(t+\tau_i) c(t) \cos(2\pi f_c t + \theta_i) \end{aligned} \tag{4.8}$$

The despread Jammer signal reaches the receiver with no data bit, PN or Walsh sequence. The jammer interference is simply a tone located in the middle of the satellite receiver bandwidth spectrum. Since the jammer cannot synchronize itself with the receiver, a phase difference between the jammer and receiver (θ_j) is inevitable.

$$J_1(t) = \sqrt{2P_j} \cos(2\pi f_c t + \theta_j)\, c(t)\, w_1(t) \tag{4.9}$$

2. The Demodulated Signal, $y_2(t)$

A demodulated signal is simply obtained by applying the modulation tone, which is coherent detection. The subscript "2" indicates demodulation in our notation.

$$\begin{aligned} y_2(t) &= y_1(t) \cos(2\pi f_c t) \\ &= \left(I_1(t) + g_1(t) + n_1(t) + V_1(t) + J_1(t) \right) \cos(2\pi f_c t) \\ &= I_2(t) + g_2(t) + n_2(t) + V_2(t) + J_2(t) \end{aligned} \tag{4.10}$$

Now, let's calculate each of the components of the demodulated signal to obtain the decision statistic, Y

Despread and modulated information bits, $I_2(t)$:

$$\begin{aligned} I_2 &= \sqrt{2P_1}\, b_1(t)\cos(2\pi f_c t)\cos(2\pi f_c t) \\ &= \frac{\sqrt{2P_1}}{2} b_1(t)\left(1+\cos(4\pi f_c t)\right) \end{aligned} \tag{4.11}$$

where

$\cos^2(2\pi f_c t) = \frac{1}{2}\left(1+\cos(4\pi f_c t)\right)$.

Despread and modulated co-channel interference, $g_2(t)$:

$$g_2(t) = \sum_{\substack{k=0 \\ k\neq 1}}^{K-1} \frac{\sqrt{2P_k}}{2} b_k(t)\, w_k(t)\, w_1(t)\left(1+\cos(4\pi f_c t)\right) \tag{4.12}$$

Despread and modulated AWGN

$$n_2(t) = n(t)\, c(t)\, w_1(t)\cos(2\pi f_c t) \tag{4.13}$$

Despread and demodulated inter-VSAT interference

$$V_2(t) = \sum_{i=1}^{M}\sum_{k=0}^{K_i-1} \frac{\sqrt{2P_{ik}}}{2} b_{ik}(t+t_i)\, w_{ik}(t+t_i) w_1(t)\, c_i(t+t_i) c(t)\cos(2\pi f_c t + \theta_i)\cos(2\pi f_c t)$$

where

$$\begin{aligned} &\cos(2\pi f_c t + \theta_i)\cos(2\pi f_c t) \\ &= \frac{1}{2}\left[\cos\theta_i - \cos(4\pi f_c t)\cos\theta_i + \sin(4\pi f_c t)\sin\theta_i\right] \end{aligned}$$

$$\begin{aligned} V_2(t) = \sum_{i=1}^{M}\sum_{k=0}^{K_i-1} \frac{\sqrt{2P_{ik}}}{2} b_{ik}(t+t_i)\, w_{ik}(t+t_i) w_1(t)\, c_i(t+t_i) c(t) \\ \left[\cos\theta_i - \cos(4\pi f_c t)\cos\theta_i + \sin(4\pi f_c t)\sin\theta_i\right] \end{aligned} \tag{4.14}$$

Despread and modulated jammer interference

$$J_2(t) = \sqrt{2P_j}\, c(t)\, w_1(t)\cos(2\pi f_c t + \theta_j)\cos(2\pi f_c t)$$
$$= \frac{\sqrt{2P_j}}{2} c(t)\, w_1(t)\left[\cos\theta_j - \cos(4\pi f_c t)\cos\theta_j + \sin(4\pi f_c t)\sin\theta_j\right] \quad (4.15)$$

3. The Decision Statistic

Decision statistic, Y, can be modeled as Gaussian random variable with a mean value of $\overline{Y}$ and variance of x. The variance of Y will be introduced in next section.

$$Y = \int_0^T y_2(t)\, dt$$
$$Y = \int_0^T I_2(t)\, dt + \underbrace{\int_0^T g_2(t)\, dt}_{g} + \underbrace{\int_0^T n_2(t)\, dt}_{n} + \underbrace{\int_0^T V_2(t)\, dt}_{V} + \underbrace{\int_0^T J_2(t)\, dt}_{J} \quad (4.16)$$

where,

g : Co-channel Interference,

$$g = \int_0^T \sum_{\substack{k=0 \\ k\neq 1}}^{K-1} \frac{\sqrt{2P_k}}{2} b_k(t)\, w_k(t)\, w_1(t)\left(1+\cos(4\pi f_c t)\right) dt \quad (4.17)$$

n : Additive White Gauissian Noise

$$h = \int_0^T n(t)\, c(t)\, w_1(t)\cos(2\pi f_c t)\, dt \quad (4.18)$$

V : Inter-VSAT Interference

$$V = \int_0^T V_2(t)dt$$

$$= \int_0^T \sum_{i=1}^{M} \sum_{k=0}^{K_i-1} \frac{\sqrt{2P_{ik}}}{2} b_{ik}(t+t_i)\, w_{ik}(t+t_i) w_1(t) c_i(t+t_i) c(t)$$

$$\left[\cos j_i - \cos(4p\ f_c t)\cos j_i + \sin(4p\ f_c t)\sin j_i\right] dt$$

$$= \sum_{i=1}^{M} \sum_{k=0}^{K_i-1} \cos j_i \frac{\sqrt{2P_{ik}}}{2} \int_0^T b_{ik}(t+t_i) w_{ik}(t+t_i) w_1(t) c_i(t+t_i) c(t)\, dt$$

In reference [3] $a_{ik}(t+t_i)$ and $d_1(t)$ are given as

$$\begin{aligned} a_{ik}(t+t_i) &= b_{ik}(t+t_i) w_{ik}(t+t_i) c_i(t+t_i) \\ d_1(t) &= w_1(t) c(t) \end{aligned} \tag{4.19}$$

$$V = \sum_{i=1}^{M} \sum_{k=0}^{K_i-1} \frac{\sqrt{2P_{ik}}}{2} \cos j_i \int_0^T a_{ik}(t+t_i) d_1(t)\, dt \tag{4.20}$$

J : Jammer Interference

$$J = \int_0^T \frac{\sqrt{2P_j}}{2} c(t)\, w_1(t) \left[\cos j_j - \cos(4p\ f_c t)\cos j_j + \sin(4p\ f_c t)\sin j_j\right] dt$$

Since the multiplication of f_c and t was selected as the integer multiplier, the integration of cos and sine functions over a period is always zero.

$$J = \frac{\sqrt{2P_j}}{2} \cos j_j \int_0^T c(t)\, w_1(t)\, dt \tag{4.21}$$

a. Mean Value of Decision Statistic, Y

$$\overline{Y} = E\left\{ \int_0^T I_2(t)\, dt + \int_0^T g_2(t)\, dt + \int_0^T n_2(t)\, dt + \int_0^T V_2(t)\, dt + \int_0^T J_2(t)\, dt \right\} \tag{4.22}$$

$$\overline{Y} = E\left\{\int_0^T I_2(t)\,dt\right\} + \cancel{E\{g\}} + \cancel{E\{n\}} + \cancel{E\{V\}} + \cancel{E\{J\}}$$
$$= E\left\{\int_0^T I_2(t)\,dt\right\}$$

$$\overline{Y} = \int_0^T \frac{\sqrt{2P_1}}{2} b_1(t)\left(1+\cos(4p\ f_c t)\right)dt$$
$$= \pm\frac{\sqrt{2P_1}}{2}T \tag{4.23}$$

Since the multiplication of f_c and t was selected as the integer multiplier, the integration of cos and sine functions over a period is always zero. Likewise, integration of $b_1(t)$ over a period is ± 1. Because the number of ones and minus ones are assumed to be equal.

4. Variance of Decision Statistic, Y

The variance of our decision statistic is the sum of the variances of our co-channel interference term and noise plus jammer term, which are assumed to be independent:

$$\begin{aligned} Var\{x\} &= Var\{g\} + Var\{n\} + Var\{V\} + Var\{J\} \\ &= E\{g^2\} + E\{n^2\} + E\{V^2\} + E\{J^2\} \end{aligned} \tag{4.24}$$

a. Variance of co-channel interference

$$Var\{g\} = E\{g^2\}$$
$$= E\left\{\left(\int_0^T \sum_{\substack{k=0\\k\neq 1}}^{K-1} \frac{\sqrt{2P_k}}{2} b_k(t)\,w_k(t)\,w_1(t)\left(1+\cos(4p\ f_c t)\right)dt\right)^2\right\} \tag{4.25}$$
$$= 0$$

Because $\int_0^T w_1(t)\ w_k(t) = 0$ where $k \neq 1$.

b. Variance of AWGN

$$
\begin{aligned}
Var\{n\} &= E\{n^2\} \\
&= E\left\{\int_0^T n(t)c(t)w_1(t)\cos(2\pi f_c t)dt \int_0^T n(\lambda)c(\lambda)w_1(\lambda)\cos(2\pi f_c \lambda)d\lambda\right\} \\
&= E\left\{\int_0^T\int_0^T n(t)n(\lambda)c(t)c(\lambda)w_1(t)w_1(\lambda)\cos(2\pi f_c t)\cos(2\pi f_c \lambda)dt\,d\lambda\right\}
\end{aligned}
\tag{4.26}
$$

We assume that $n(t)$ is a wide-sense stationary white noise process. The autocorrelation of the wide-sense stationary white noise process was defined in reference [16] as

$$
E\{n(t)n(\lambda)\} = \frac{N_0}{2}\delta(t-\lambda). \tag{4.27}
$$

so,

$$
\begin{aligned}
Var\{n\} &= \frac{N_0}{2}\int_0^T c^2(t)\,w_1^2(t)\frac{1}{2}\left(1+\cos(4\pi f_c t)\right)dt \\
&= \frac{N_0 T}{4}
\end{aligned}
\tag{4.28}
$$

c. Variance of the Inter-VSAT Interference

$$Var\{V\} = E\{V^2\}$$

$$Var\{V\} = \sum_{i=1}^{M}\sum_{k=0}^{K_i-1} E\left\{\left(\frac{\sqrt{2P_{ik}}}{2}\cos(\theta_i)\int_0^T a_{ik}(t+\tau_i)d_1(t)\,dt\right)^2\right\}$$

$$Var\{V\} = \sum_{i=1}^{M}\sum_{k=0}^{K_i-1} E\left\{\frac{P_{ik}}{2}\cos^2(\theta_i)\int_0^T a_{ik}(t+\tau_i)d_1(t)dt\int_0^T a_{ik}(\lambda+\tau_i)d_1(\lambda)\,d\lambda\right\}$$

$$Var\{V\} = \frac{P_{ik}}{4}\sum_{i=1}^{M}\sum_{k=0}^{K_i-1}\int_0^T\int_0^T \underbrace{E\{a_{ik}(t+\tau_i)a_{ik}(\lambda+\tau_i)\}}_{b(t-\lambda)}\underbrace{E\{d_1(t)d_1(\lambda)\}}_{b(t-\lambda)}dt\,d\lambda$$

$$Var\{V\} = \frac{P_{ik}}{4}\sum_{i=1}^{M}\sum_{k=0}^{K_i-1}\int_0^T\int_0^T b^2(t-l)\,d\,t\,dl$$

Let's apply transformation of limits and variables of the integral

$$u = t - l \qquad \rightarrow u + v = 2t$$
$$v = t + l \qquad \rightarrow u - v = -2\,l$$
$$t = \frac{1}{2}(u+v)$$
$$l = \frac{1}{2}(v-u)$$
$$J_{tl} = \det\begin{bmatrix}\frac{\partial t}{\partial u} & \frac{\partial l}{\partial u}\\ \frac{\partial t}{\partial v} & \frac{\partial l}{\partial v}\end{bmatrix} = \det\begin{bmatrix}\frac{1}{2} & -\frac{1}{2}\\ \frac{1}{2} & \frac{1}{2}\end{bmatrix} = 1/2$$

After applying transformation

$$Var\{V\} = \sum_{i=1}^{M}\sum_{k=0}^{K_i-1}\frac{P_{ik}}{4}\int_{-T}^{T}\int_{|u|}^{2T-|u|} b^2(u)\,J_{tl}\,du\,dv$$
$$= \sum_{i=1}^{M}\sum_{k=0}^{K_i-1}\frac{P_{ik}}{4}\int_{0}^{T}\int_{|u|}^{2T-|u|} b^2(u)\,du\,dv$$
$$= \sum_{i=1}^{M}\sum_{k=0}^{K_i-1}\frac{P_{ik}}{4}\int_{0}^{T} b^2(u)\,(2T-2u)\,du$$

$$b(u) = \begin{Bmatrix}1-\frac{Nu}{T} & |u| \le T_c\\ 0 & otherwise\end{Bmatrix}$$

$$Var\{V\} = \sum_{i=1}^{M}\sum_{k=0}^{K_i-1}\frac{P_{ik}}{4}\int_0^{T/N}\left(1-\frac{2Nu}{T}+\frac{N^2u^2}{T^2}\right)(2T-2u)\,du$$
$$= \sum_{i=1}^{M}\sum_{k=0}^{K_i-1}\frac{P_{ik}}{4}2\left(Tu-Nu^2+\frac{N^2u^3}{3T}-\frac{u^2}{2}+\frac{2Nu^3}{3T}-\frac{N^2u^4}{4T^2}\right)\Bigg|_0^{T/N} \qquad (4.29)$$
$$= \sum_{i=1}^{M}\sum_{k=0}^{K_i-1}\frac{P_{ik}}{4}\left(\frac{2T^2}{3N}-\frac{T^2}{6N^2}\right)$$
$$= \sum_{i=1}^{M}\sum_{k=0}^{K_i-1}\frac{P_{ik}}{2}\left(\frac{T^2}{3N}\right) \qquad for\ N \gg 1$$

d. Variance of Jammer Interference

The derivation of the jammer interference is not much different from the inter-VSAT interference,

$$\begin{aligned} Var\{J\} &= E\{J^2\} \\ &= E\left\{\frac{P_j}{2}\cos^2(j_j)\int_0^T\int_0^T c(t)w_1(t)c(l)w_1(l)dtdl\right\} \end{aligned} \tag{4.30}$$

Recall from (4.19) $d_1(t) = w_1(t)c(t)$.

$$\begin{aligned} Var\{J\} &= \frac{P_j}{4}\int_0^T\int_0^T E\{d_1(t)d_1(l)\}dtdl \\ &= \frac{P_j}{4}\int_0^T\int_0^T b(t-l)\,dtdl \\ &= \frac{P_j}{4}\int_{-T}^{T}\int_{|u|}^{2T-|u|} b(u)J_{tl}\,dvdu \\ &= \frac{P_j}{4}\int_0^T\int_{|u|}^{2T-|u|} b(u)\,dvdu \\ &= \frac{P_j}{4}\int_0^T 2b(u)(T-u)\,du \end{aligned}$$

$$\begin{aligned} b(u) &= 1-\frac{u}{T_c} \\ &= 1-\frac{Nu}{T} \quad \text{where } T_c = \frac{T}{N} \end{aligned}$$

$$\begin{aligned} Var\{J\} &= \frac{P_j}{2}\int_0^{T/N}\left(T-u-Nu+\frac{Nu^2}{T}\right)du \\ &= \frac{P_j}{2}\left(Tu-\frac{u^2}{2}-\frac{Nu^2}{2}+\frac{Nu^3}{3T}\Big|_0^{T/N}\right) \\ &= \frac{P_j}{2}\left(\frac{T^2}{N}-\frac{T^2}{2N^2}-\frac{NT^2}{2N^2}+\frac{NT^3}{3TN^3}\right) \end{aligned}$$

$$= \frac{P_j}{2}\left(\frac{T^2}{N} - \frac{T^2}{2N^2} - \frac{T^2}{2N} + \frac{T^2}{3N^2}\right)$$
$$= \frac{P_j}{2}\left(\frac{T^2}{2N} - \frac{T^2}{6N^2}\right) \tag{4.31}$$
$$= \frac{P_j T^2}{4N} \qquad for\ N \gg 1$$

5. Signal-to-Noise Plus Interference Plus Jamming Ratio

$$Var\{x\} = Var\{n\} + Var\{V\} + Var\{J\}$$
$$= \frac{N_0 T}{4} + \sum_{i=1}^{M}\sum_{k=0}^{K_i-1}\frac{P_{ik}T^2}{6N} + \frac{P_j T^2}{4N} \tag{4.32}$$

$$SINR = \frac{\overline{Y^2}}{Var\{x\}}$$
$$= \frac{\frac{P_1 T^2}{2}}{\frac{N_0 T}{4} + \sum_{i=1}^{M}\sum_{k=0}^{K_i-1}\frac{P_{ik}T^2}{6N} + \frac{P_j T^2}{4N}} \tag{4.33}$$

$$SINR = \frac{1}{\frac{N_0}{2TP_1} + \sum_{i=1}^{M}\sum_{k=0}^{K_i-1}\frac{P_{ik}}{3NP_1} + \frac{P_j}{2NP_1}} \tag{4.34}$$

P_{ik} and P_1 can be considered equal. The incoming transmissions from the channel that is meant to be detected and the interfering channels are assumed to have the same power because the size of the footprint on earth is very small relative to the geostationary satellite altitude.

$$SINR = \frac{1}{\frac{N_0}{2TP_1} + \frac{M(K-1)}{3N} + \frac{P_j T}{2NP_1 T}}$$

$$P_j T = E_I$$

$$P_1 T = E_b$$

$$\frac{E_b}{E_I} = SJR(\text{SignaltoJamRatio})$$

$$\frac{E_b}{N_0} = SNR(\text{SignaltoNoiseRatio})$$

$$SINR = \frac{1}{\frac{1}{2(SNR)} + \frac{M(K-1)}{3N} + \frac{1}{2N(SJR)}} \tag{4.35}$$

6. Performance Analysis with Convolutional Encoding

Proakis states in reference [4] that

$$\begin{aligned} P_2(d) &< Q(\sqrt{(d\,(SINR)\,R)} \\ &< Q\left(\sqrt{\frac{d\,R}{\frac{1}{2\,(SNR)} + \frac{M(K-1)}{3N} + \frac{1}{2N\,(SJR)}}}\right) \\ &< Q\left(\sqrt{\frac{d}{\frac{1}{2R\,(SNR)} + \frac{M(K-1)}{3NR} + \frac{1}{2NR\,(SJR)}}}\right) \end{aligned} \tag{4.36}$$

where R is the code rate.

The reference [4] defines the Q function as in (4.37).

$$Q(x) = \frac{1}{2} erfc(\frac{x}{\sqrt{2}}) \tag{4.37}$$

And finally, the upper bound for the probability of bit error for the Spread Spectrum, DS-CDMA BPSK VSAT system is [4]

$$P_b < \sum_{d=d_{free}}^{\infty} b_d P_2(d) \tag{4.38}$$

Where the set of b_d s represents the distance spectrum of the code.

Therefore,

$$P_b < \sum_{d=d_{free}}^{\infty} b_d Q\left(\sqrt{\frac{d}{\frac{1}{2R(SNR)} + \frac{M(K-1)}{3NR} + \frac{1}{2NR(SJR)}}}\right) \tag{4.39}$$

The probability of bit error equation (4.39) was plotted by using a Matlab® simulation. The tone jammer Matlab® simulation calculates the probability of bit error for different code rates and for a different number of active channels. The results were plotted as probability of bit error, (P_b), versus signal-to-noise ratio, E_b/N_0. The simulation was run for four different signal power-to-spreading factor times jammer power ratio (P_1/NP_j). According to the simulation results, as the number of users increase, the performance of the VSAT system becomes worse. The performance was never acceptable for any traffic intensity and for jammer powers for the coding rates of $1/8$, $1/16$ and $1/32$.

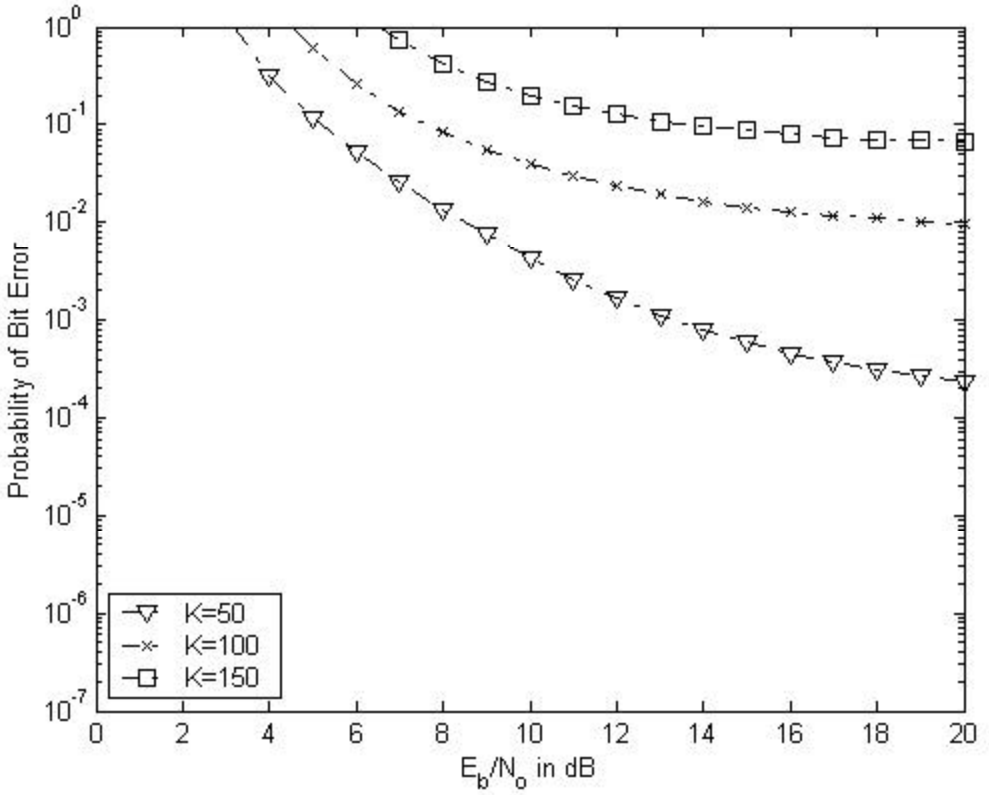

Figure 19. Performance of VSAT System with the Code Rate of 1/16 in Low Power Jammer Condition P_1 / NP_j =15 dB.

Even in a low power jammer scenario, the codes specified above perform very unsatisfactorily.

Except for those code rates specified above, in every other code rate, the system can support data communication only for a low number of active users in adverse tone jammer conditions (P_1 / NP_j = 5 dB). N is chosen 256 as previously explained. Additionally, lower codes $3/4$ and $2/3$ did not perform well for severe jamming. Even though the best performance was obtained for the code rate of $1/120$, there is little performance difference between the code rate $1/3$ and $1/120$. For a signal-to-noise ratio of 15 dB and for a high number of active channels, code $1/120$ can perform 0.5 dB better than the code rate of 1/3 for an expense of 40 times less bit rate. Therefore code rate 1/3 is the best solution in a severe tone-jamming situation.

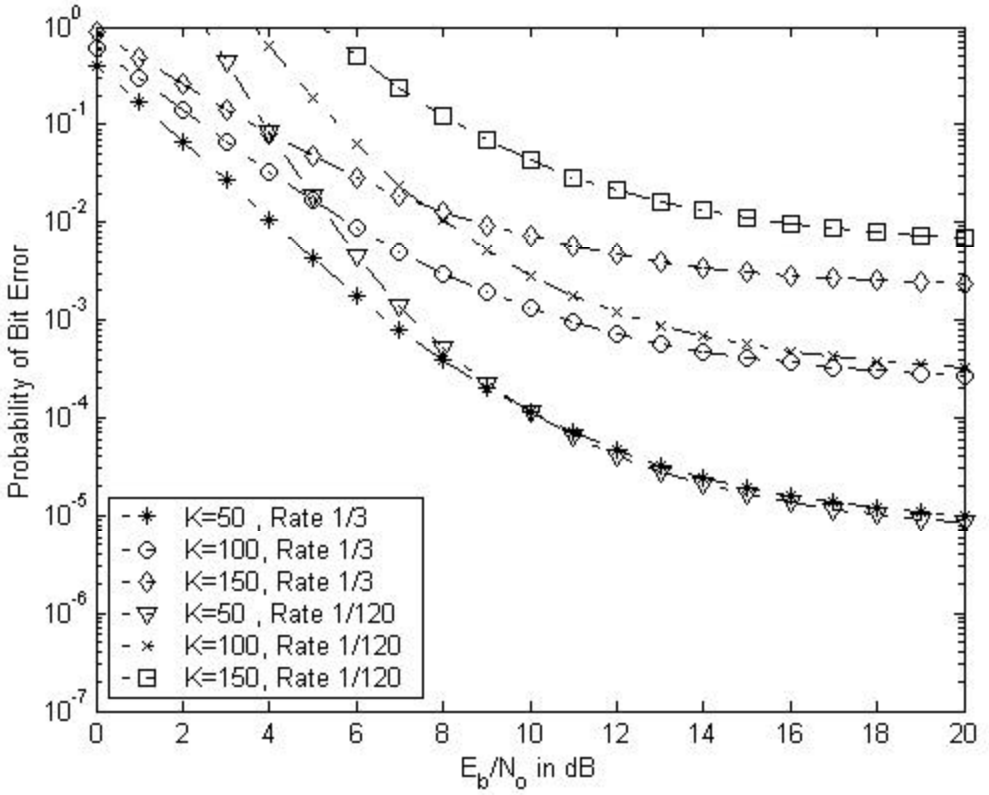

Figure 20. Comparison of Code Rates of $1/3$ and $1/120$ for P_1 / NP_j = 5 dB

As the jammer power changes from adverse to upper moderate (P_1 / NP_j =10 dB), even code rates $3/4$ and $2/3$ performed well for low loads. However, code 1/3 still had the best optimal performance relative to code rate 1/128. Even for the best performance, the probability of bit error was insignificant than 7×10^{-4}. The change in performance for different code rates was not too much for heavy loads. This result confirms that as the traffic intensity increases, the co-channel interference and inter-VSAT interference are the dominant factors on performance. For example, performance differences between the code rates of $1/3$ and $1/120$ diminish as the number of active channels increases in Figure 20.

In low jammer effect conditions (P_1 / NP_j =15 dB or P_1 / NP_j =20 dB), the probability of bit error always remains under 10^{-7} up to 100 active channels. The best performing code rates almost support reliable voice communication in a weak jammer scenario.

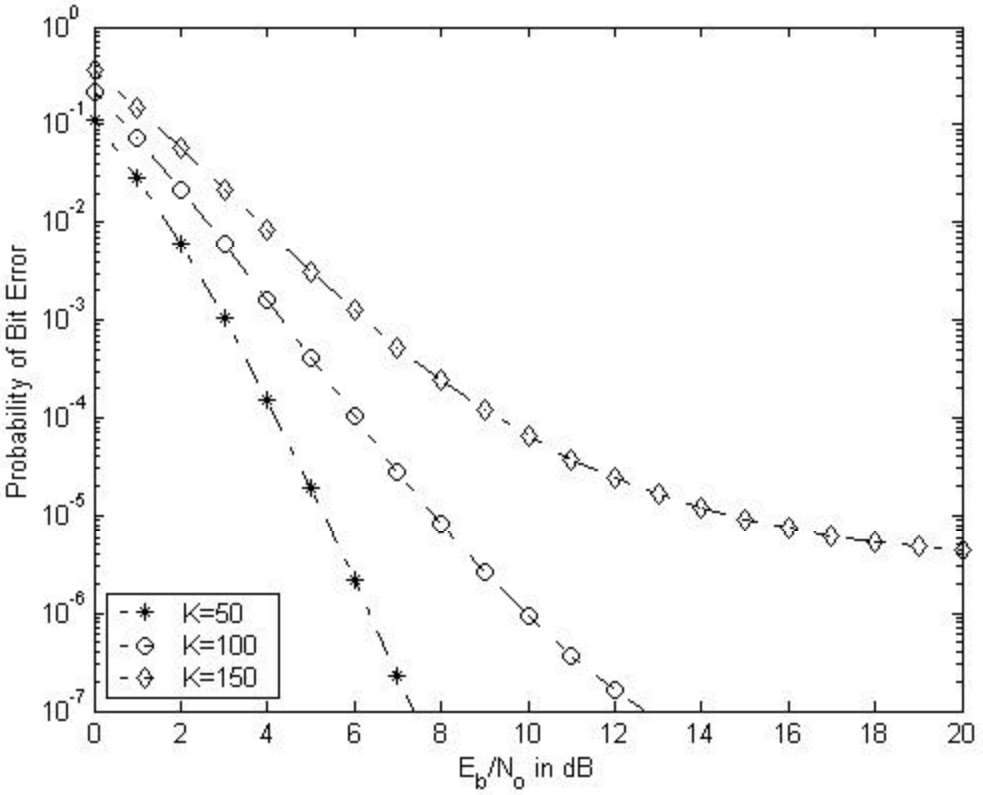

Figure 21. Performance of Code Rate $1/3$ for $P_1 / NP_j = 15\,dB$.

Finally, the proposed VSAT system can sustain data communication for all jammer-included scenarios via code rate 1/3. Voice communication can only be conducted with less active channels in moderate jammer power condition.

B. PERFORMANCE ANALYSIS WITH PULSE JAMMER

Pulse jamming is one of the most effective ECM techniques. In this technique, the jammer is activated for a short period of time and paused for the rest of the period. The variable duty cycle of the pulse jammer (r) influences the performance of the targeted communication system. The pulse jammer duty cycle (r) is a function of the ratio of the signal power to the total jammer power (P/J) [2]. The lower duty cycle requires much bandwidth compared with the higher duty cycle, jamming the wider part of the operational bandwidth of the communication system. The jammer can even jam the entire bandwidth of the target system by applying the necessary duty cycle. On the other hand, since the jammer has limited power, the power spectral density over the unit band would be decreased as the jammed band increases. As illustrated in Figure 16 at the beginning of Chapter IV, the total area under the power spectral density curve for a jammer will always be the same, regardless of the applied duty cycle or the jammed portion of the whole band.

This situation causes the jammer operator to consider a tradeoff between the duty cycle and power spectral density pair to force the target communication system to perform as poorly as possible.

As previously mentioned, the jammer is activated for a fraction of the total period. The variance of interference that is received by the satellite receiver changes accordingly. Jammed bits, $r_{l,1}$ can be modeled as Gaussian random variable with mean $-\sqrt{E_c}$ volts and a variance of, [16]

$$s_I^2 = \frac{(K-1)E_c}{3N_c} + \frac{N_0}{2} + \frac{N_I}{2r} \tag{4.40}$$

where

N_I = PSD of Jammer

r = Jammer pulse duty cycle $(0 \le r \le 1)$

Unjammed bits, $r_{l,2}$ are also modeled as Gaussian random variable with mean $-\sqrt{E_c}$ as well and a variance of,

$$s^2 = \frac{(K-1)E_c}{3N_c} + \frac{N_0}{2} \tag{4.41}$$

The combination of two Gauissian variables, Y, received by the satellite receiver is expected to be Gaussian again. This property was depicted as in (4.42) in reference [4].

$$P_2(d \mid i) = P\left\{\sum_{l=1}^{d} r_l \geq 0\right\} \tag{4.42}$$

Because every received bit is not jammed, the equation above can be adapted for the noise jammer as,

$$P_2(d \mid i) = P\left\{\left(\sum_{l=1}^{i} r_{l,1} + \sum_{l=i+1}^{d} r_{l,2}\right) \geq 0\right\} \tag{4.43}$$

In this expression, we assumed that i of the total d bits a period are jammed and $(d-i)$ bits are unjammed.

1. Mean and Variance of Gaussian Random Variable Y [4]

$$M_y = \sum_{l=1}^{i} m_i \tag{4.44}$$

where $m_i = -\sqrt{E_c}$

The jammer will not affect the mean of the Y.

$$M_y = \sum_{l=1}^{i} -\sqrt{E_c} + \sum_{l=i+1}^{d} -\sqrt{E_c} = \sum_{l=1}^{d} -\sqrt{E_c}$$
$$= -d\sqrt{E_c}$$

The variance of r.v. Y is affected by the jammer as explained previously. Therefore we must define the variance according to the duty cycle of the jammer.

$$
\begin{aligned}
s_y^2 &= \sum_{l=1}^{n} s_l^2 \\
&= \sum_{l=1}^{i} s_I^2 + \sum_{l=i+1}^{d} s^2 \\
&= i s_I^2 + (d-i) s^2
\end{aligned}
\tag{4.45}
$$

Let's substitute the s_I^2 and s^2 found in equations (4.40) and (4.41) respectively.

$$
s_y^2 = i\left(\frac{(K-1)E_c}{3N_c} + \frac{N_0}{2} + \frac{N_I}{2r}\right) + (d-i)\left(\frac{(K-1)E_c}{3N_c} + \frac{N_0}{2}\right)
$$

$$
= \cancel{\frac{i(K-1)E_c}{3N_c}} + \cancel{\frac{iN_0}{2}} + \frac{iN_I}{2r} + \frac{d(K-1)E_c}{3N_c} - \cancel{\frac{i(K-1)E_c}{3N_c}} + \frac{dN_0}{2} - \cancel{\frac{iN_0}{2}}
$$

$$
s_y^2 = \frac{iN_I}{2r} + \frac{d(K-1)E_c}{3N_c} + \frac{dN_0}{2} \tag{4.46}
$$

$$
N_c = \frac{T_c}{T_{chip}} = RN \quad also \quad E_c = RE_b
$$

$$
Therefore; \frac{E_c}{N_c} = \frac{\cancel{R}E_b}{\cancel{R}N} = \frac{E_b}{N}
$$

N was described as the total spreading factor. The total spreading factor, N is fixed to an integer, 256, which is the multiplication of the spreading factor due to the coding and spreading factor due to the PN sequence spreading. In this case, the equation (4.46) can be simplified as follows:

$$
s_y^2 = \frac{iN_I}{2r} + \frac{d(K-1)E_b}{3N} + \frac{dN_0}{2} \tag{4.47}
$$

2. Conditional Probability of Error, $P_2(d \mid i)$

Since we know the exact amount of jammed bits (i) to calculate variance, the conditional probability of error $P_2(d \mid i)$ can be calculated by the following equation [4].

$$P_2(d \mid i) = Q\left(\sqrt{\frac{\overline{M_y^2}}{s_y^2}}\right)$$

$$= Q\left(\sqrt{\frac{d^2 E_c}{\frac{i N_I}{2r} + \frac{d(K-1)E_c}{3N_c} + \frac{d N_0}{2}}}\right)$$

$$= Q\left(\sqrt{\frac{d^{\not 2} \not{E_c}}{\frac{i N_I}{2r d E_c} + \frac{\not{d}(K-1)\not{E_c}}{3\not{d}\not{E_c} N_c} + \frac{\not{d} N_0}{2\not{d} E_c}}}\right)$$

$$= Q\left(\sqrt{\frac{d}{\frac{i N_I}{2r d E_c} + \frac{(K-1)}{3N_c} + \frac{N_0}{2E_c}}}\right) \tag{4.48}$$

3. First-Event Error Probability, $P_2(d)$

The First-Event Error Probability, $P_2(d)$ can be found using binomial distributions. Jamming occurs with the probability of r and not being jammed occurs with the probability of $(1-r)$. In reference [5], PMF of X for the binomial random variable X is given as:

$$P_X(x) = \begin{cases} \binom{n}{x} p^x (1-p)^{(n-x)} & x = 0,1,...,n \\ 0 & otherwise \end{cases} \tag{4.49}$$

Similarly, in reference [6] $P_2(d)$ was defined as

$$P_2(d) = \sum_{i=0}^{\infty} \binom{d}{i} r^i (1-r)^{d-i} P_2(d \mid i). \tag{4.50}$$

4. Performance Analysis with Convolutional Encoding

The probability of bit error with convolutional encoding was given in (4.38) in the tone jammer performance section.

$$\begin{aligned} P_b &= \sum_{d=d_{free}}^{\infty} b_d P_2(d) \\ &= \sum_{d=d_{free}}^{\infty} b_d \sum_{i=0}^{d} \binom{d}{i} r^i (1-r)^{d-i} P_2(d \mid i) \\ &= \sum_{d=d_{free}}^{\infty} b_d \sum_{i=0}^{d} \binom{d}{i} r^i (1-r)^{d-i} Q\left(\sqrt{\frac{d}{\frac{i N_I}{2 r d E_c} + \frac{(K-1)}{3 N_c} + \frac{N_0}{2 E_c}}} \right) \end{aligned} \tag{4.51}$$

We can use the same simplification for the term inside the Q function, as we did for the tone jamming.

$$P_b = \sum_{d=d_{free}}^{\infty} b_d \sum_{i=0}^{d} \binom{d}{i} r^i (1-r)^{d-i} Q\left(\sqrt{\frac{d}{\frac{i\,N_I}{2d\,r\,RE_b} + \frac{(K-1)}{3RN} + \frac{N_0}{2RE_b}}} \right)$$

$$= \sum_{d=d_{free}}^{\infty} b_d \sum_{i=0}^{d} \binom{d}{i} r^i (1-r)^{d-i} Q\left(\sqrt{\frac{d}{\frac{i}{2d\,r\,R\frac{E_b}{N_I}} + \frac{(K-1)}{3RN} + \frac{1}{2R\frac{E_b}{N_0}}}} \right)$$

where $\frac{E_b}{N_I} = SJR$ *and* $\frac{E_b}{N_0} = SNR$

$$P_b = \sum_{d=d_{free}}^{\infty} b_d \sum_{i=0}^{d} \binom{d}{i} r^i (1-r)^{d-i} Q\left(\sqrt{\frac{d}{\frac{i}{2d\,r\,R(SJR)} + \frac{(K-1)}{3RN} + \frac{1}{2R(SNR)}}} \right) \quad (4.52)$$

The pulse jammer simulation shows similar results to the noise jammer simulation. Pulse jammer Matlab® simulation calculates the probability of bit error for different code rates, for different numbers of active channels and for different duty cycles of the jammer (r). The results were plotted as the probability of bit error (P_b) versus the signal-to-noise ratio for each signal-to-jam ratio (E_b / J_0) of 5, 10, 15 and 20 dB. According to the simulation results, some common patterns were revealed: For example, as the code rate increases, system performance becomes more unyielding against the variable jammer duty cycle. Deterministically, for the code rate of $1/4$, the performance of the VSAT system decreases 12 dB as the duty cycle of the jammer decreased to 0.01 from 0.1 for $E_b/N_0 = 10\,dB$, $E_b/J_0 = 15\ dB$ and $K = 100$ active users (Figure 22).

However, for the same configuration, the VSAT performance decreases only 0.5 dB for the code rate of $1/32$ (Figure 23). For this reason, choosing a lower code rate would be more appropriate to eliminate this capability of the jammer. The expected

common pattern for all the results was that the performance of the VSAT system becomes worse as the number of users increase due to increasing interference from co-channels.

A rate span of $3/4$ to rate $1/128$ has been studied to observe the effects of a code rate over the probability of bit error. Code rates up to $1/4$, do not affect the P_b severely. Figure 24 and Figure 25 illustrate the performance difference between the code rate of $1/2$ and $1/64$ for $E_b/J_0 = 15\ dB$. However, for the rates $1/8$, $1/16$ and $1/32$ the performances are not acceptable for all signal-to-jam ratios, similar to the case in tone jamming. Then, for the rates $1/64$, $1/128$ performance increases again. For instance, for the rate of $1/128$ the results are slightly better than for the rate $1/2$ for $r = 1$ (Figure 26). However, rate $1/128$ cannot provide data rates as high as rate $1/2$ can. The spectrum distances algorithm used to obtain the b_d coefficients gives perfect results for the rates of $1/20$, $1/40$, $1/60$ and $1/120$. Because of these perfect spectral distance coefficients, rate $1/20$ performs better than rate $1/16$. Moreover, rate $1/60$ and $1/120$ perform better than rates $1/64$ and $1/128$ respectively.

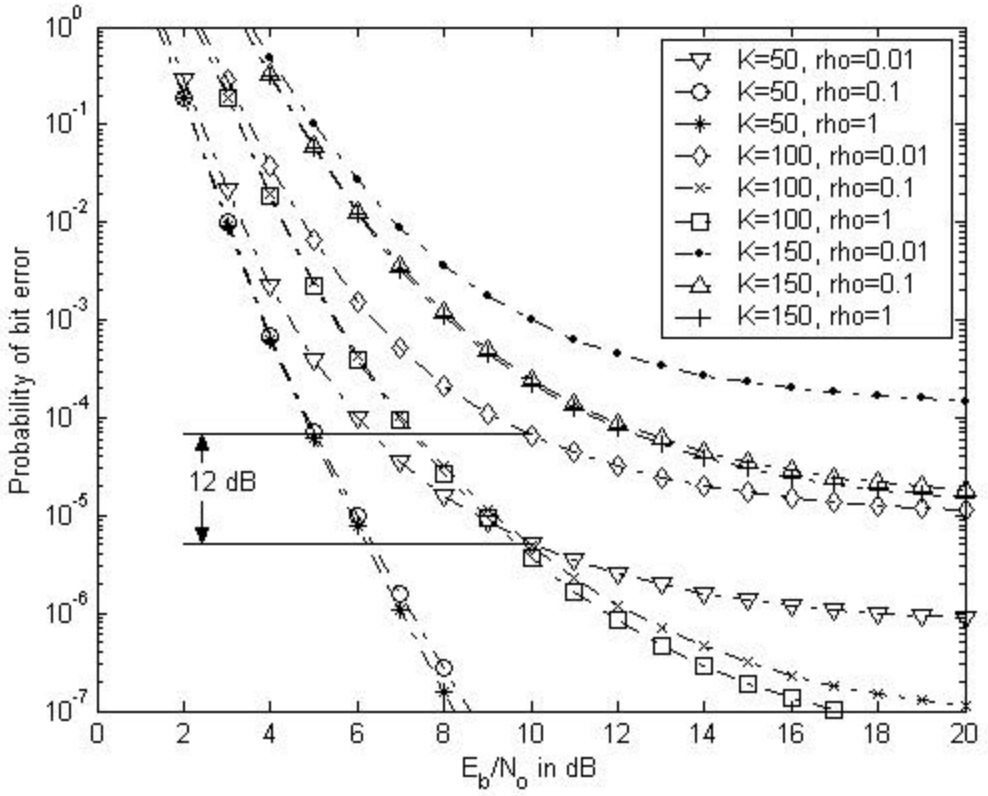

Figure 22. Pulse Jammer Effect for Code Rate $1/4$ and $E_b / J_0 = 15\,dB$

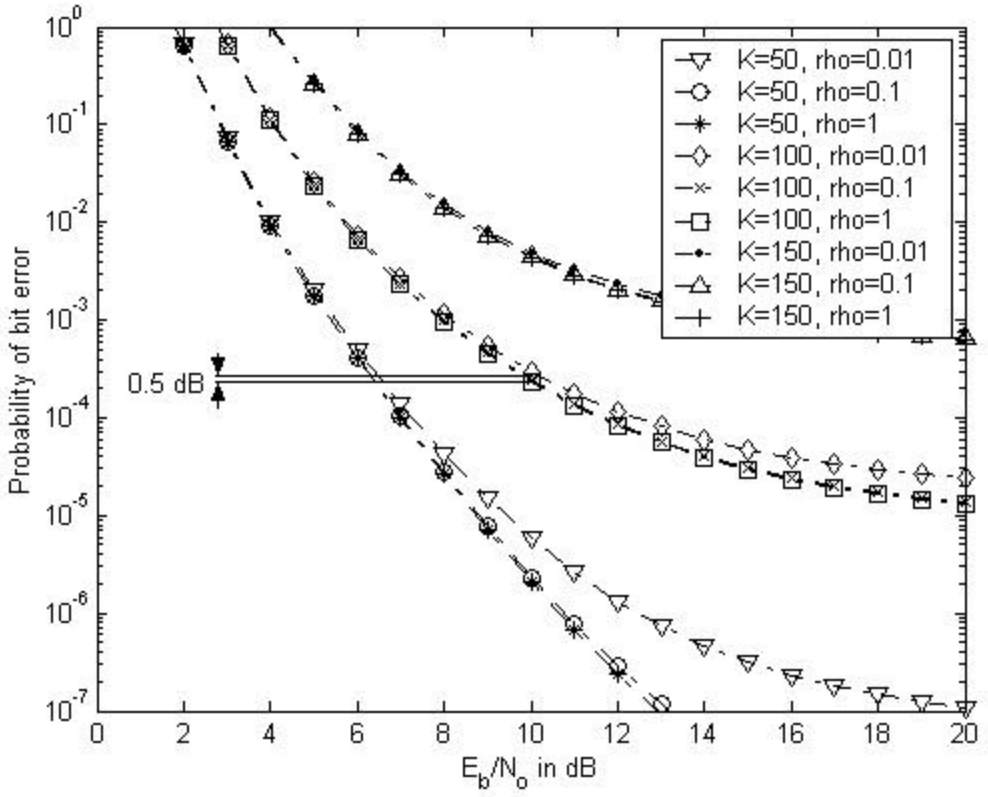

Figure 23. Pulse Jammer Effect for Code Rate $1/32$ and $E_b / J_0 = 15\,dB$

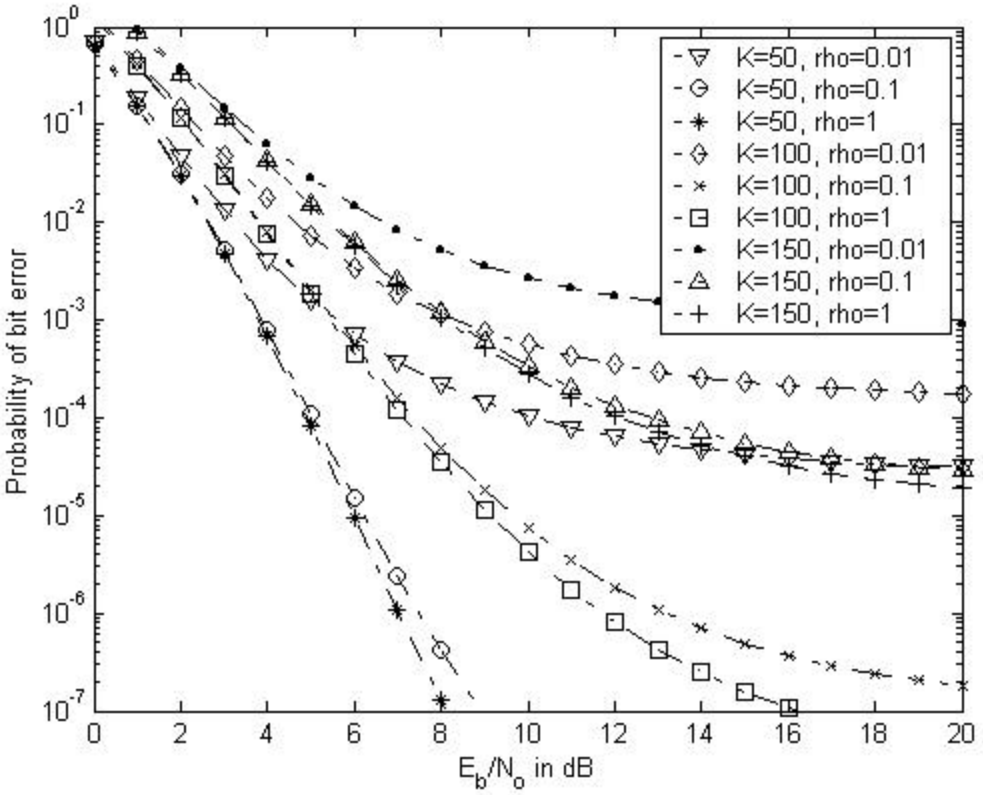

Figure 24. Pulse Jammer Effect for Code Rate $1/2$ and $E_b / J_0 = 15\,dB$

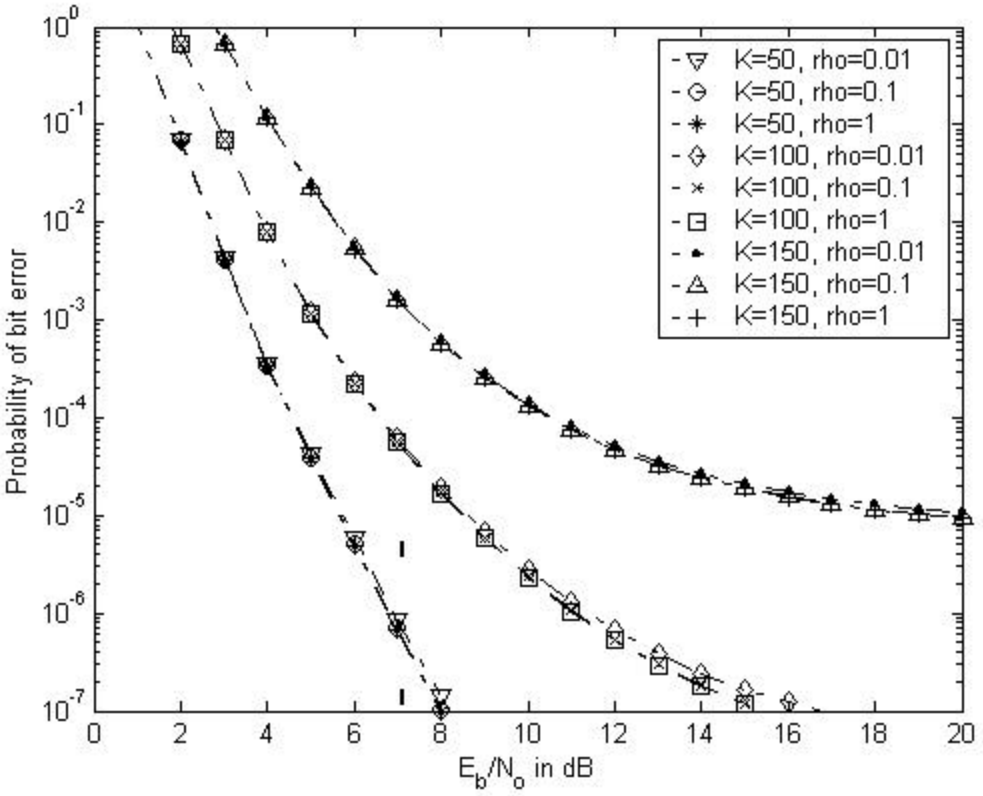

Figure 25. Pulse Jammer Effect for Code Rate $1/64$ and $E_b / J_0 = 15\,dB$

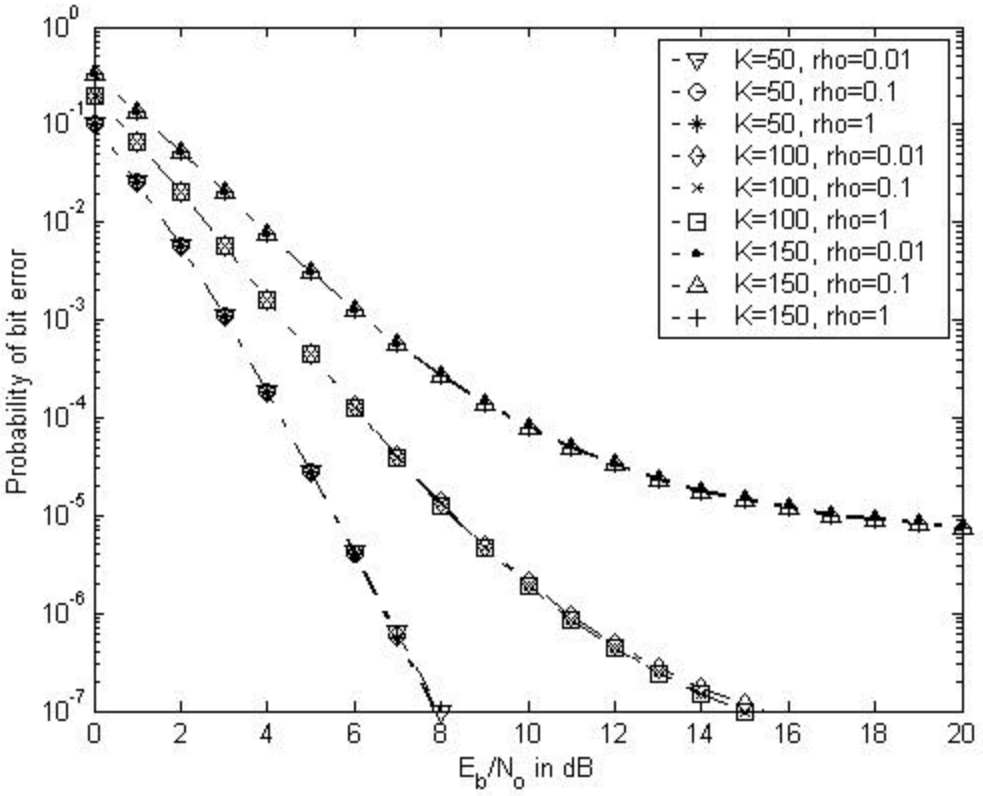

Figure 26. Pulse Jammer Effect for Code Rate $1/128$ and $E_b / J_0 = 15\,dB$

The simulation results also showed that performance is mostly affected by intrasystem interference for E_b / J_0 values greater than 15 dB. In other words, co-channel interference or inter-VSAT interference is more effective than jammer interference for this situation.

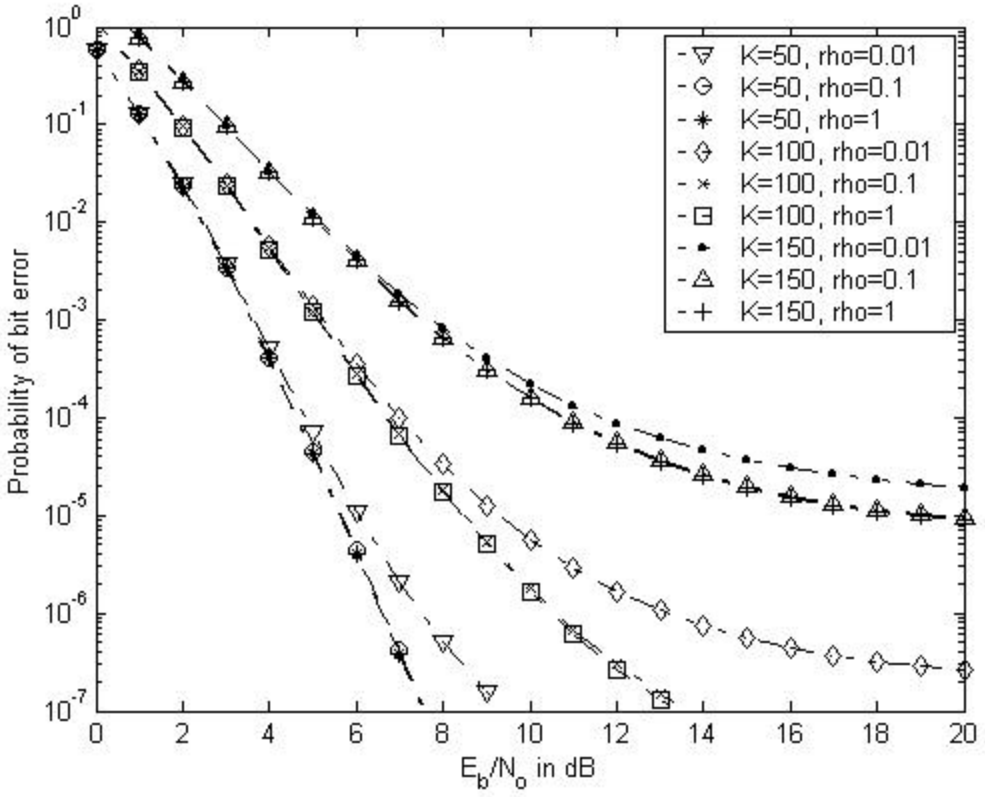

Figure 27. Pulse Jammer Effect for Code Rate $1/2$ and $E_b / J_0 = 20\,dB$

The differences in performance curves between the Figure 24 and Figure 27 illustrate that changing in performance for the different channel densities decreases as the E_b / J_0 ratio increases.

Figure 28 introduces that any signal-to-jam ratio below 5 dB is not enough for a reliable communication. In this illustration, one of the best performing code rate, $1/3$, was used.

High code rates such as $1/3$ or $1/4$ guarantees reliable communication for all reasonable signal-to-jam conditions (Figure 29). But as the number of active channels

increases (over 150), the small duty cycles of the jammer can increase the probability of bit error over 10^{-4}.

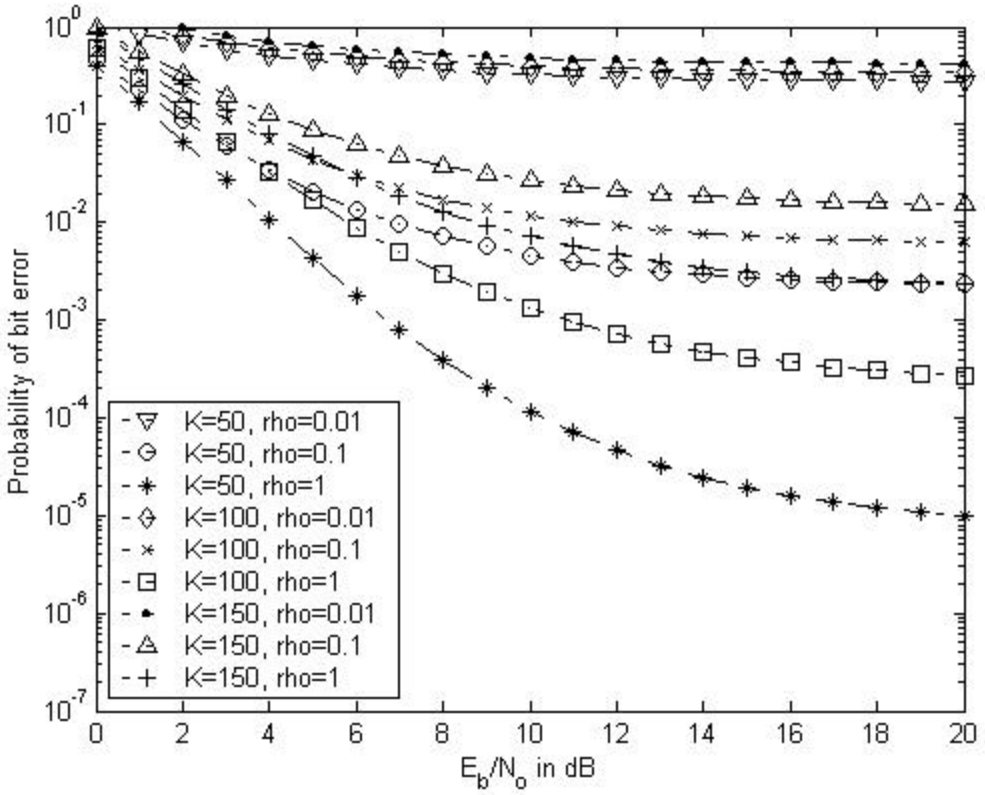

Figure 28. Pulse Jammer Effect for Code Rate $1/3$ and $E_b / J_0 = 5\,dB$

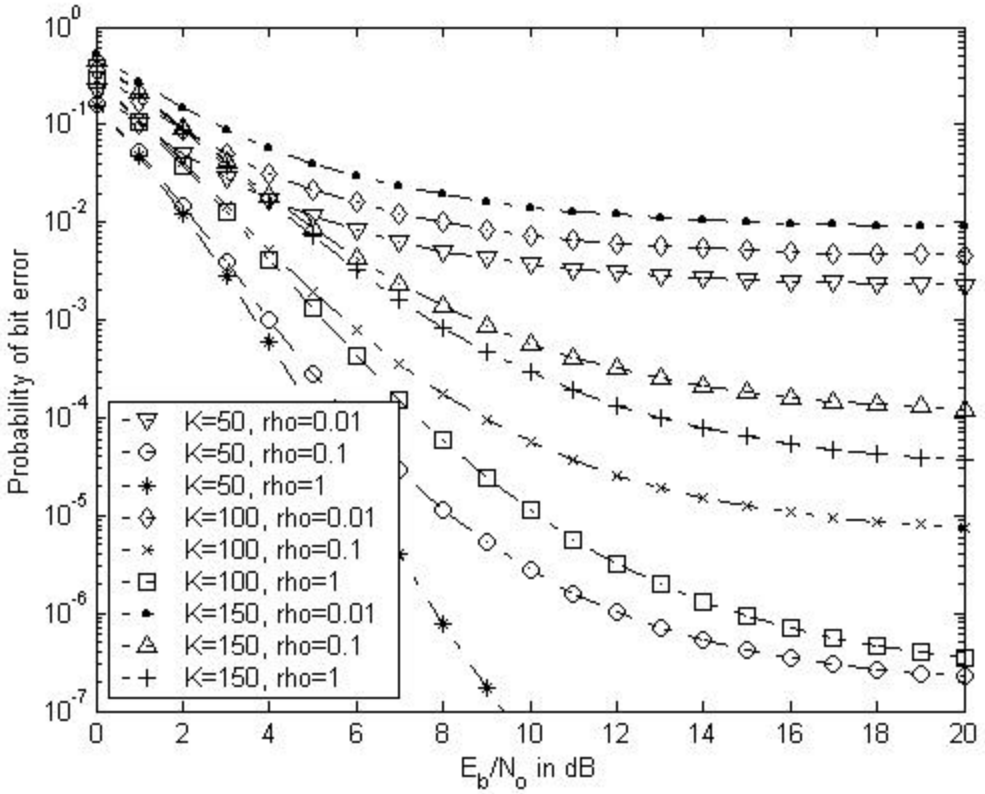

Figure 29. Pulse Jammer Effect for Code Rate $1/3$ and $E_b / J_0 = 10\,dB$

In a jammer free scenario, the rate $1/2$ or $1/3$ would perform best, enabling all users to communicate with high data rates. After the jammer appears in the same scenario, the VSAT system would switch to a higher code rate but to a lower data rate until communication could be accomplished efficiently. Code $1/20$ or $1/40$ would be the most optimum code rates for moderate jamming. If the jamming is more severe, rate $1/120$ must be used with only data communication. The reason voice communication cannot be used is that the proposed VSAT system has a limited bandwidth.

C. SUMMARY

In this chapter, we modeled the VSAT system by defining the similarities and differences between cellular and satellite communication. We have used properties of the Walsh function and the autocorrelation function of PN sequences through the whole analysis

Two types of jammer effects were analyzed with Matlab® simulations. We have looked for a proposed probability of bit error corresponding to the minimum and maximum signal-to-noise ratios, which were introduced in Chapter II. As a result of these simulations, the superiority of the pulse jammer over the tone jammer was revealed. In other words, the proposed VSAT system is more resistive to the tone jammer than it is to the pulse jammer. Considering the hostile side, the worst case for the enemy pulse jammer ($r = 1$) was as effective as the tone jammer. The lower duty cycles of the pulse jammer decreased the performance of our VSAT system dramatically.

Both jammer capabilities can prevent the platforms from making secure voice communication. Except under severe conditions, data communication can be supported most of the time. As a countermeasure, decreasing the system bit rate, planning the necessary EMCON measures in an operation or decreasing the number of communicating channels would even increase the performance more. As previously mentioned in the Rain Loss section of Chapter II, increasing the output power of VSAT increases the signal-to-noise ratio. Therefore, better performance is obtained. Even though, the overall spreading factor was fixed to 256 in this thesis, increasing processing gain by using more PN chips per bit increase the durability against enemy jammer effects.

V. CONCLUSIONS

In this thesis, we have presented the tools for a DS-CDMA Spread Spectrum communication system using forward error correcting mechanism and analyze the performance of proposed system by using those tools.

The main goal in Chapter II was calculating the minimum signal-to-noise ratio that our system can support. Initially, we defined the term VSAT and other orbital mechanics parameters. Then we decided on the proposed VSAT system requirements. By using the physical sizes, distances and power limitations, a link budget analysis was made. The worst-case scenario was considered in this analysis assuming a friendly platform at the edge of the satellite footprint and the enemy jammer at the best place to minimize our system performance. The link budget analysis presented the minimum and maximum signal-to-noise ratios that can be established at the satellite receiver. The difference between the minimum and maximum signal-to-noise ratios has been calculated by the rain loss analysis.

In Chapter III, we examined the algebraic properties of Walsh functions and PN sequences that will help us to figure out how to minimize jammer effects and friendly interference on our system. The Walsh functions consisted of orthogonal sequences, which support full coverage between sequences. We also presented the extended orthogonality that ensures the orthogonality between every channel in a VSAT. The PN sequences were used to spread out our frequency spectrum, reducing the power spectral density, and minimizing the jammer effects. Afterwards, we introduced the convolutional forward error correction coding, which lets the system perform better with a low signal-to-noise ratio.

The performance analyses were introduced in Chapter IV. The performance analyses were considered both for tone jammer and pulse jammer. First of all, we developed a signal-to noise plus interference ratio and the probability of bit error for our DS-CDMA satellite system by using Gaussian approximation. We used Gaussian approximation to define median and variances of random variable Y. For both jammer

cases, co-channel interference, inter-VSAT interference, Additive White Gaussian Noise and Jammer Interference were considered as variances of Y. We introduced Forward Error Correction in the form of convolutional encoding with soft-decision decoding into our uplink model and developed an upper bound on the probability of bit error [3].

We used Matlab® to run the simulations. The simulation results for both jammer types revealed that the proposed VSAT uplink system could accommodate the data or voice communication within reasonable limits. The performance plots were given in probability of bit error versus signal-to-noise ratio for the different jammer powers and the number of active channels. We used the obtained minimum signal-to-noise ratio in Chapter II to decide whether system performance was sufficient or insufficient. The following results are valid for both pulse and tone jammer.

- As the number of active channels increases, the probability of bit error increases.
- As the jammer power increases, the probability of bit error increases.
- There was no direct correlation between the code rate and the system performance.
- The performances of code rates of $1/8$, $1/16$ and $1/32$ were unacceptable.
- The code rates $1/3, 1/120$ and $1/128$ were best performing code rates.
- The code rate $1/3$ introduces most efficient performance and bit rate pair.

Additionally, some results were subject to specific jammer types.

- The worst case for enemy pulse jammer ($r = 1$) affected VSAT uplink as badly as the tone jammer.
- As the duty cycle of pulse jammer decreases, the probability of bit error increases.
- As the pulse jammer power decreases, the effect of changing duty cycle decreases. In other words, for the high E_b / J_0 values effects of tone jammer and pulse jammer are almost the same.

Finally, we must recall that we never gave up considering the worst-case scenario in our analysis. In the real word we would expect better performance from our VSAT system. Also, changing antenna size, increasing the VSAT power or decreasing bit rate can always empower the VSAT system against unpredictable and variable jammer capabilities.

THIS PAGE INTENTIONALLY LEFT BLANK

LIST OF REFERENCES

[1]. August Golden Jr., *Radar Electronic Warfare*, Newyork, Newyork. American Institute of Aeronautics and Astronautics, Inc., 1987.

[2]. Peterson, L.P., Ziemer, R.E., Borth, D.E., Introduction to Spread Spectrum Communications, Upper Saddle River, New Jersey. Prentice Hall,Inc., 1995

[3]. Tighe, J.E., *Modelling And Analysis of Cellular CDMA Forward Channel*, Naval Postgraduate School, Monterey, California, March 2001.

[4]. Proakis, J.G., Digital Communications, 4th ed., Boston, Massachusetts. WCB/McGrawhill, 1993.

[5]. Yates, R.D., Goodman, D.J., *Probability and Stochastic Processes*, Newyork, John Wiley & Sons. Inc., 1999.

[6]. Robertson, R.C., Ha T., "Error Probabilities of Fast Frequency-Hopped FSK with Self-Normalization Combining in a Fading Channel with Partial-Band Interference," *IEEE Journal on Selected Areas in Communications, Vol. 10, No. 4, May 1992.*

[7]. http://www.eurasiasat.com/

[8]. Roddy, D., *Satellite Communications*, 3rd ed., New York. McGraw Hill, 2001

[9]. Ippolito, L.J.Jr.,Radiowave *Propagation in Satellite Communications*, Van Nostrand Reinhold CompanyInc.,1986.

[10]. Saam ,T. J, "The Economic benefits of VSAT's", *IEEE International Conference on, 1990* Pages:370-375 vol.2., 1990.

[11]. European Telecommunication Standards Institute ETS 300 159, December 1992

[12]. RUPAR, Michael, *Satellite VSAT networking using CDMA*, Naval Research Laboratory, 19

[13]. Lee, J.S., L.E. Miller, CDMA Systems Engineering Handbook, Artech House, 1998

[14]. http://www.cdmaonline.com

[15]. Yigit, U., *Performance Analysis of a CDMA VSAT System with Convolutional and Reed-Solomon Coding*., Naval Postgraduate School, Monterey, California, September 2002.

[16]. Rappaport, T.S., *Wireless Communications*,2nd ed.,Prentice Hall, 2002.

[17]. Elbert, B.R., *The Satellite Communication Ground Segment and Earth Station Handbook*, Artech House, 2000.

INITIAL DISTRIBUTION LIST

1. Defense Technical Information Center
   8725 John J. Kingman Rd., STE 0944
   Ft. Belvoir, VA 22060-6218

2. Dudley Knox Library
   Naval Postgraduate School
   411 Dyer Rd.
   Monterey, CA 93943-5121

3. Deniz Kuvvetleri Komutanligi
   Personel Daire Baskanligi
   Bakanliklar 06410
   Ankara, TURKEY

4. Deniz Harp Okulu Kütüphanesi
   Tuzla 34942
   Istanbul, TURKEY

5. Dan C. Boger, Chairman, Code IS
   Naval Postgraduate School
   Monterey, CA 93943-5121

6. Prof. Tri HA
   Naval Postgraduate School
   Monterey, CA 93943-5121

7. Prof. Herschel H. Loomis Jr
   Naval Postgraduate School
   Monterey, CA 93943-5121